ENGINEERING LIBRARY

RR

SEP 20 1949

# THE AERONAUTICAL QUARTERLY

Volume I AUGUST 1949 Part II

CONTENTS

Displacements of a Linear Elastic System Under a Given Transient Load — *D. Williams*

Skin Friction in the Laminar Boundary Layer in Compressible Flow — *A. D. Young*

The Measurement of Gas Turbine Combustion Efficiency by Gas Analysis — *L. J. Richards* and *J. C. Street*

A Simplified Theory of "Simple Waves" — *A. Ghaffari*

LONDON
ROYAL AERONAUTICAL SOCIETY
4 HAMILTON PLACE W1

10/-

# THE AERONAUTICAL QUARTERLY


*Editorial Board*

W. G. A. PERRING, F.R.Ae.S. (*Chairman*)

Dr. H. ROXBEE COX, D.I.C., F.R.Ae.S., F.I.Ae.S.

Professor S. GOLDSTEIN, F.R.S., F.R.Ae.S.

Sir RICHARD SOUTHWELL, M.A., LL.D., F.R.S., F.R.Ae.S.

G. H. DOWTY, F.R.Ae.S. (Chairman of the JOURNAL Committee of the Royal Aeronautical Society)

J. SMITH, C.B.E., F.R.Ae.S., A.M.I.Mech.E. (Chairman of the Technical Board and Executive Committee of the Society of British Aircraft Constructors)

---

*Editorial Executives*

Captain J. Laurence Pritchard, Hon.F.R.Ae.S., Hon.F.I.Ae.S.
Joan Bradbrooke, A.R.Ae.S. Dr. D. M. A. Leggett, A.F.R.Ae.S.

---

*Editorial Referees*

*Aerodynamics*

(a) *General*

Prof. L. Bairstow
Dr. G. P. Douglas
Prof. A. A. Hall
Sir B. Melvill Jones
Mr. D. Keith-Lucas
Dr. N. A. V. Piercy
Mr. W. G. A. Perring
Mr. E. F. Relf
Mr. R. Smelt
Mr. E. J. Richards

(b) *Field Motion*

Mr. A. Fage
Prof. S. Goldstein
Dr. L. Howarth
Dr. J. W. Maccoll
Dr. J. H. Preston
Mr. L. F. G. Simmons
Mr. H. B. Squire
Sir Geoffrey Taylor
Prof. G. Temple
Mr. A. D. Young

(c) *Stability and Control*

Mr. L. W. Bryant
Mr. S. B. Gates
Mr. G. T. R. Hill
Mr. H. B. Irving
Mr. G. H. Lee
Mr. M. B. Morgan

*Helicopters and Propellers*

Dr. J. A. J. Bennett
Mr. L. G. Fairhurst
Mr. R. Hafner
Capt. R. N. Liptrot

*Instrumental and Electrical Equipment*

Dr. G. E. Bairsto
Mr. I. Bowen
Mr. G. W. H. Gardner
Mr. C. S. Hudson
Mr. A. N. Ikens
Mr. C. N. Jaques
Mr. F. W. Meredith
Mr. H. C. Pritchard

*Aircraft Design*

Mr. R. Boorman
Mr. R. M. Clarkson
Mr. A. N. Clifton
Mr. W. S. Farren
Mr. H. H. Gardner
Mr. H. Knowler
Mr. W. E. W. Petter
Mr. F. H. Pollicutt
Mr. A. E. Russell
Mr. R. S. Stafford

*Radio and Radar*

Mr. J. F. Atherton
Mr. B. G. Gates
Mr. R. L. Smith Rose
Dr. A. M. Uttley
Sir Robert Watson Watt

*Aviation Medicine*

Dr. A. Buchanan Barbour

*Meteorology*

Prof. D. Brunt
Mr. J. K. Hardy
Prof. P. A. Sheppard

*Aircraft Propulsion*

Mr. H. Constant
Sir A. H. Roy Fedden
Dr. S. Hooker
Mr. P. Lloyd
Dr. A. W. Morley
Dr. E. S. Moult
Mr. N. S. Muir
Mr. F. Nixon
Mr. F. M. Owner
Dr. D. Pye
Mr. H. Sammons
Prof. O. A. Saunders

*Air Transport*

Mr. P. G. Masefield
Mr. N. E. Rowe
Mr. K. T. Spencer
Mr. W. Tye

*Aircraft Accessories*

Mr. W. C. Clothier
Mr. H. G. Conway
Mr. G. H. Dowty
Mr. R. Graham

*Vibration and Flutter*

Prof. A. R. Collar
Prof. W. J. Duncan
Mr. R. A. Frazer
Mr. J. Hanson

*Performance*

Mr. H. Davies
Mr. D. R. Newman
Mr. A. H. Yates

*Structures*

Mr. A. C. Brown
Mr. H. L. Cox
Mr. D. J. Farrar
Mr. H. Grinsted
Dr. H. Roxbee Cox
Mr. W. S. Hemp
Mr. H. B. Howard
Mr. E. D. Keen
Mr. F. A. Kerry
Dr. D. M. A. Leggett
Pro. R. L. Lickley
Prof. A. J. Sutton Pippard
Prof. A. G. Pugsley
Dr. S. C. Redshaw
Mr. R. H. Sandifer
Sir Richard Southwell

*Fuels and Oils*

Mr. E. L. Bass
Mr. J. W. Drinkwater
Prof. F. H. Garner
Prof. W. E. Garner
Dr. K. E. W. Ridler
Dr. C. G. Williams

*Materials*

Prof. L. Aitchison
Dr. N. P. Allen
Prof. N. F. Mott
Mr. L. Rotherham
Dr. H. Sutton
Dr. C. Sykes

*Flight Testing*

Mr. P. A. Hufton
Mr. E. T. Jones
Mr. S. Scott Hall
Mr. H. L. Stevens

# DISPLACEMENTS OF A LINEAR ELASTIC SYSTEM UNDER A GIVEN TRANSIENT LOAD

by

D. WILLIAMS, D.Sc., M.I.Mech.E., A.F.R.Ae.S.
*(Structures Department, Royal Aircraft Establishment)*

## PART I

### 1. INTRODUCTION

A method is described for obtaining the displacements (and hence the stresses) of a linear elastic system under a given transient load in a more accurate and more expeditious manner than is possible by the standard method. For simplicity, no account is taken of damping forces in describing the method.

The method is of interest to engineers and others who require to obtain numerical answers to problems of the type described above. It depends upon the fact that in many practical cases of transient loads the inertia forces in the series of normal modes of an elastic system converge rapidly, compared with the series of "normal" loadings in terms of which the spatial distribution of the applied load can be expressed.

The first application of the method to a practical problem was made by the author in a Royal Aircraft Establishment[1] report in which the effects of landing and of gust forces on the wing stresses of an aeroplane were investigated. The essence of the new approach was subsequently described in a paper read at the Sixth International Congress of Applied Mechanics (Paris, September 1946), and the form of the argument used there is repeated in Sections 2-5. For readers familiar with vibration theory the formal presentation of the argument in those Sections requires no amplification; but the practical usefulness of the method is so great, particularly for aeronautical engineers, that it was thought worthwhile to expand the argument, and to show, by means of a simple example, precisely how the saving in labour and gain in accuracy is brought about. In the matter of accuracy, it will also be made clear why, theoretically, the standard method is incapable of giving an accurate solution and why complete accuracy is achieved by the modified approach.

---

Paper received December 1948.
[The Aeronautical Quarterly, Vol. 1, August 1949]

## 2. BASIS OF STANDARD METHOD

The argument runs as follows:—

Let a force $P(x) . F(t)$ be a transient load applied to a continuous elastic system (with therefore an infinite number of degrees of freedom), where $P(x)$ represents the spatial *distribution* (assumed constant with time) of the applied load and $F(t)$ its variation with time.

It is well known that the function $P(x)$ can be expanded in a series of normal loadings each having a distribution identical with that of the inertia loading in the corresponding normal mode. Thus let

$$P(x)=L_1(x)+L_2(x)+\ldots\ldots+L_n(x)+\ldots\ldots \quad . \quad . \quad (1)$$

and therefore

$$P(x).F(t)=F(t)[L_1(x)+\ldots\ldots+L_n(x)\ldots\ldots] \quad . \quad . \quad (1a)$$

## 3. STANDARD PROCEDURE

The standard procedure is to calculate the displacements caused by each of the terms on the right hand side of (1*a*) independently of the others, beginning with $F(t)\,L_1(x)$ and continuing one by one until it is considered that a close enough approximation to the total effect has been reached.

The disadvantage of this procedure is seen immediately when, for example, only the first two or three resonance modes of the system are excited, the remaining modes having displacements corresponding only to the static application of the corresponding loadings. These remaining modes have to be considered up to a term $F(t)\,L_r(x)$ where $r$ is high enough to make

$$\sum_{n=1}^{r} L_n(x)=P(x)$$

to a reasonable degree of accuracy.

If $P(x)$ is a concentrated load $r$ is likely to be fairly large, making it necessary to evaluate a correspondingly large number of terms.

## 4. SUGGESTED PROCEDURE

To obviate the difficulty indicated above we note that, in the absence of the corresponding inertia forces, the displacement of the system in the $n^{th}$ mode at

every instant is equal to the statical displacement appropriate to the $n^{th}$ normal loading, *i.e.* to the force $F(t) \cdot L_n(x)$ at that instant. If we add to this the displacement corresponding to the appropriate inertia loading $f_n(t) \cdot L_n(x)$ we shall have the resultant displacement of the system in the $n^{th}$ mode, the function $f(t)$ representing the time variation of the inertia loading $L_n(x)$ and being different for each mode.

The total resultant displacement at every instant is therefore that appropriate to the loadings:—

$$[F(t) \cdot L_1(x) + f_1(t) \cdot L_1(x)] + [F(t) \cdot L_2(x) + f_2(t) \cdot L_2(x)] + \quad . \quad . \qquad (2)$$

*i.e.* to $$F(t) \sum_{n=1}^{\infty} L_n(x) + \sum_{n=1}^{\infty} f_n(t) L_n(x)$$

or to $$P(x) \cdot F(t) + \sum_{n=1}^{\infty} f_n(t) \cdot L_n(x). \quad . \quad . \quad . \quad . \qquad (3)$$

Now in many practical cases the second term in (3) converges rapidly and can be evaluated with little difficulty. The first term, being the original applied load, is already known and its effect (as a static force) can be added immediately to that of the second term to give the complete behaviour of the system.

## 5. EVALUATION OF INERTIA FORCES

The inertia forces are readily obtained by the use of Duhamel's Integral. In the $n^{th}$ mode, for example, the Equivalent Static Force is given by

$$(\text{E.S.F.})_n = p_n \cdot L_n(x) \int_0^t F(t_1) \sin p_n (t - t_1)\, dt_1 \quad . \quad . \quad . \qquad (4)$$

where $(\text{E.S.F.})_n$ is the static force in the $n^{th}$ mode that gives the same displacement as the actual dynamic force $L_n(x) \cdot F(t)$ at every instant $t$ from the beginning of force application, and where $P_n$ is the circular frequency in the same mode.

Now, at every instant the Applied Force $(\text{A.F.})_n$ (*i.e.* $L_n(x) F(t)$) is resisted by an elastic force equal to $(\text{E.S.F.})_n$, but opposite in sign, and an Inertia Force $(\text{I.F.})_n$

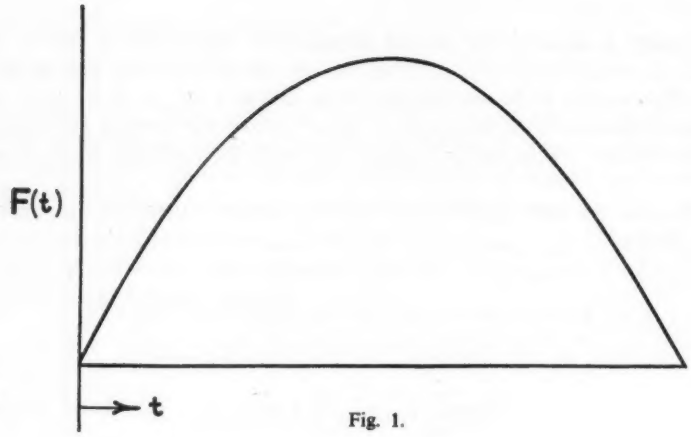


Fig. 1.

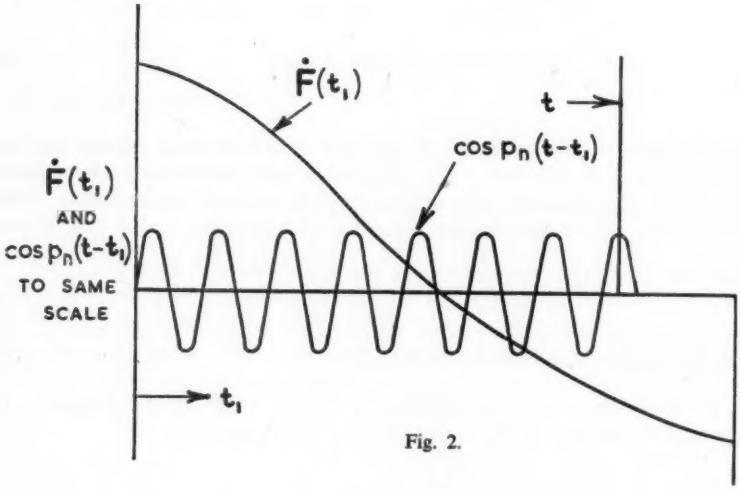


Fig. 2.

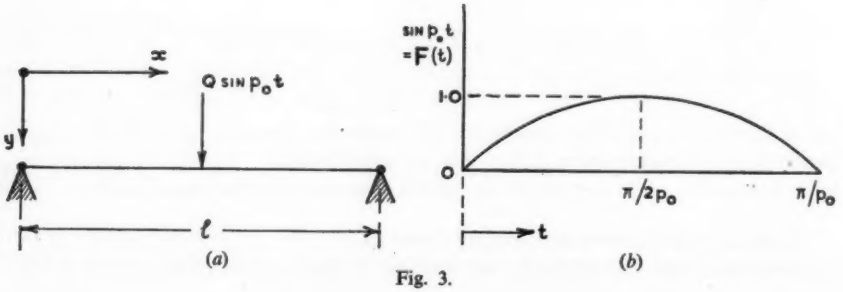


Fig. 3.

(already referred to above as $f_n(t)\,.\,L_n(x)$), and therefore

$$(\text{I.F.})_n = -(\text{A.F.})_n + (\text{E.S.F.})_n,$$

$$= L_n(x)\left[-F(t) + p_n \int_0^t F(t_1) \sin p_n(t-t_1)\, dt_1\right] . \quad . \quad . \quad (5)$$

This gives, on integration by parts,

$$(\text{I.F.})_n = L_n(x)\left[-F(t) + F(t) - \int_0^t \cos p_n(t-t_1)\, \dot{F}(t_1)\, dt_1\right]$$

$$= -L_n(x) \int_0^t \cos p_n(t-t_1)\, \dot{F}(t_1)\, dt_1 \quad . \quad . \quad . \quad . \quad . \quad (6)$$

where $\dot{F}(t_1) = \dfrac{d}{dt_1}[F(t_1)]$, and the legitimate assumption is made that the initial value of $F(t)$ is zero.

If Fig. 1 represents the curve of $F(t)$ and Fig. 2 the curve of $\dot{F}(t)$ against time $t$ it is clear that as $p_n$ increases, the value of the integral in (6) decreases (unless sharp changes of slope take place in time intervals comparable with $2\pi/p_n$).

In many practical cases $(\text{I.F.})_n$ becomes small enough to be neglected after the first few terms so that

$$\sum_{n=1}^{\infty} (\text{I.F.})_n \equiv \sum_{n=1}^{\infty} f_n(t)\,.\,L_n(x) \simeq \sum_{n=1}^{r} (\text{I.F.})_n \,. \quad . \quad . \quad . \quad (7)$$

(where $r$ is small), is a series that is readily evaluated.

*Resultant effect*

The resultant displacements, and hence the resultant stresses in the system, are therefore found at every instant from equation (3) by adding the static displacements produced by the inertia loadings to that produced by the actual applied load.

## 6. SIMPLE EXAMPLE

The convenience of the method will be appreciated if it is applied to the easy example represented by a uniform beam, simply supported at the ends, and subjected to a dynamic load applied at the mid-section and varying harmonically with time. Figs. 3 (*a*) and (*b*) together define completely the conditions of the problem, (*a*) giving the spatial distribution of the applied load, and (*b*) its variation

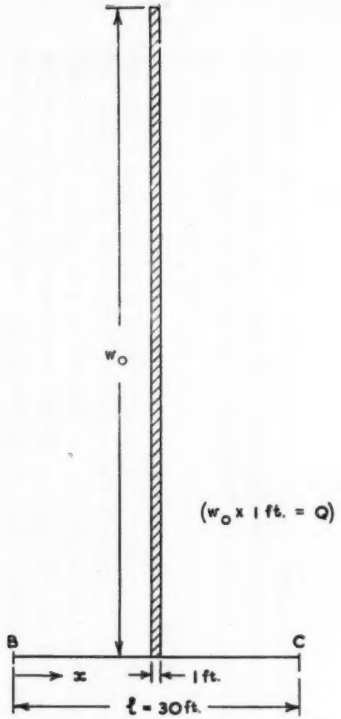


Fig. 4(*a*).
Spatial distribution of applied load $P(x)$.

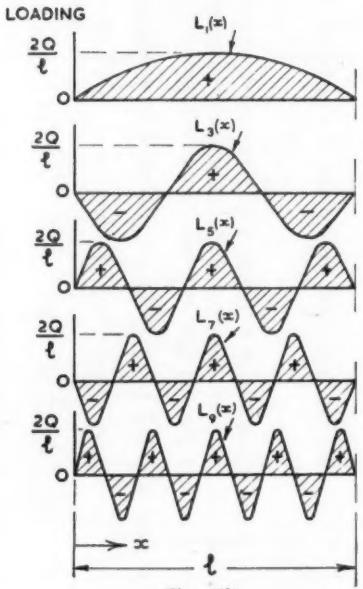


Fig. 4(*b*).
Normal component loadings whose sum approaches applied loading of Fig. 4(*a*). (1st, 3rd, 5th, 7th and 9th components shown here.)

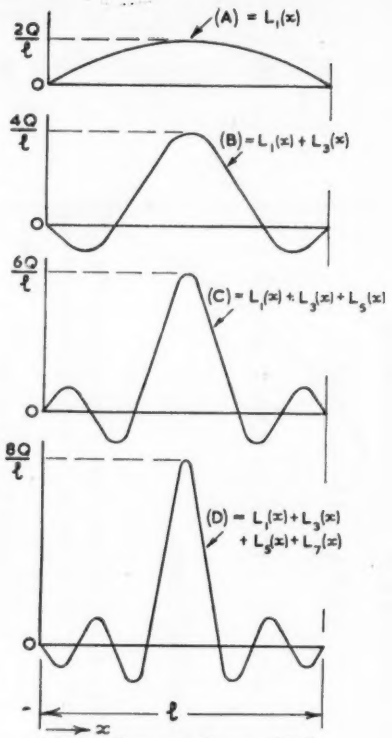


[*Note*—Compare Curve "D" loading with that of Fig. 4(*a*).]

Fig. 4(*c*).
Successive approximations to the applied loading $P(x)$ of Fig. 4(*a*) obtained by progressing along the series
$L_1(n) + L_3(x) + \ldots + L_n(x) + \ldots \infty$.

with time $F(t)$, which has here the form $\sin p_o t$. We shall consider the behaviour of the beam from zero time—representing the onset of the load—to time $\pi/p_o$ when the force is removed after passing through its maximum value $Q$ at time $\pi/2p_o$. We shall assume that the fundamental circular frequency $p_1$ of the beam is given by

$$p_1 = p_o/4, \quad . \quad . \quad . \quad . \quad . \quad . \quad . \quad (8)$$

from which, in the present case, the higher frequencies can be written down. As, by symmetry, modes that have a node at the mid-section cannot be excited by a central load, these higher frequencies are successively $9p_1$, $25p_1$, $49p_1$, $81p_1$, and so on.

Our purpose now is to follow the steps in the formal argument of Section 2 *et seq.* in terms of the concrete example before us; and this will involve certain procedures that are necessary only in the standard method of approach, but have to be included in order to demonstrate the superiority of the newer one. Referring to Fig. 4 (*a*), we shall suppose the length of the beam $BC$ to be 30 ft., and that the central load $Q$ is evenly distributed over the middle foot, which means that the load per foot over the loaded length is

$$w_o = Q \, . \quad . \quad . \quad . \quad . \quad . \quad . \quad . \quad (9)$$

The first step is to express the loading distribution $P(x)$ of Fig. 4 (*a*) as a series of "normal" loadings $L_1(x)$, $L_3(x)$, $L_5(x)$, ....., $L_n(x)$, ..... $\infty$, as indicated in equation (1) but with even values of $n$ omitted. It can be shown that in the present example

$$L_n(x) = \frac{2Q}{l} \sin(n\pi x/l) \quad . \quad . \quad . \quad . \quad . \quad (10)$$

$$(n = 1, 3, 5 \ldots).$$

so that $L_1(x)$, $L_3(x)$, ....., $L_9(x)$, ..... are given respectively by the loading diagrams of Fig. 4 (*b*). As mentioned in Section 3 it next becomes necessary in the standard method to decide how far along this series of loadings we have to proceed before we are justified in assuming that the sums of the terms give a loading that is a near enough approximation to the true loading of Fig. 4 (*a*). To judge this, we examine Fig. 4 (*c*), where the result of adding successive terms up to the fourth is shown as loadings (A), (B), (C) and (D) respectively. It is seen that, as an adequate representation of the true distribution of 4 (*a*) for the purpose of obtaining shears and bending moments, curve (D) obtained from the first four terms of the series is wholly unsatisfactory: a good many more terms have to be included before anything like a close approximation is reached. This is the point made in Section 3.

Suppose, however, that in order to operate the standard method a few more loadings are added to the series shown in 4 (*b*). The next and last step is to determine separately the dynamic effect of each of these loadings, $L_1(x)\sin p_o t$, $L_3(x)\sin p_o t$, . . . . . $L_n(x)\sin p_o t$, before adding them together to obtain the resultant.

Such a roundabout procedure is clearly wasteful when, as often happens, only one or two of the lowest modes have any appreciable dynamic effect, *i.e.* inertia forces.

In the present case the first normal loading $L_1(x)\sin p_o t$ of Fig. 4 (*b*) excites inertia forces with the same spatial distribution, but varying in magnitude and in time according to the shaded area of Fig. 5 (*a*). It is seen that at time $T_1$ the combined effect of applied and inertia loading is greater by some 25 per cent. than the maximum value of the applied first normal loading alone. In the next mode Fig. 5 (*b*) shows that the inertia loading excited by $L_3(x)\sin p_o t$ is negligibly small. For all higher modes, therefore, the normal loadings $L_5(x)\sin p_o t$, $L_7(x)\sin p_o t$, etc., excite no inertia forces, so that the applied loading is resisted in each case by the elastic forces of the system alone.

The total effect of the transient load $Q\sin p_o t$ may thus be exhibited (*cf.* equations (2) and (3)) as the sum of the following sets of forces

1. $= L_1(x)\sin p_o t + (\text{I.F.})_1$ [varying with time as in Fig. 5 (*a*)]
2. $= L_3(x)\sin p_o t +$ (negligible inertia forces)
3. $= L_5(x)\sin p_o t +$ (negligible inertia forces)

.....

*n*. $= L_n(x)\sin p_o t +$ (negligible inertia forces)

.....

or
$$(1+2+\ldots\ldots+n+\ldots\ldots\infty) = Q\sin p_o t + (\text{I.F.})_1 \quad . \quad . \quad . \quad (11)$$

In other words, the effect is the same as if the load $Q$ were a static load varying with time in accordance with the time function $\sin p_o t$, except that the inertia forces excited in the first mode (and in this case in that mode alone) have to be added as extra static forces varying with time, as shown in Fig. 5 (*a*).

By following this procedure it is seen that the necessity for considering the higher mode normal loadings represented by $L_3(x)$, $L_5(x)$, etc., is obviated and—of comparable importance—that the error involved in representing the actual distribution of the applied load by a limited number of the higher mode loadings is also avoided.

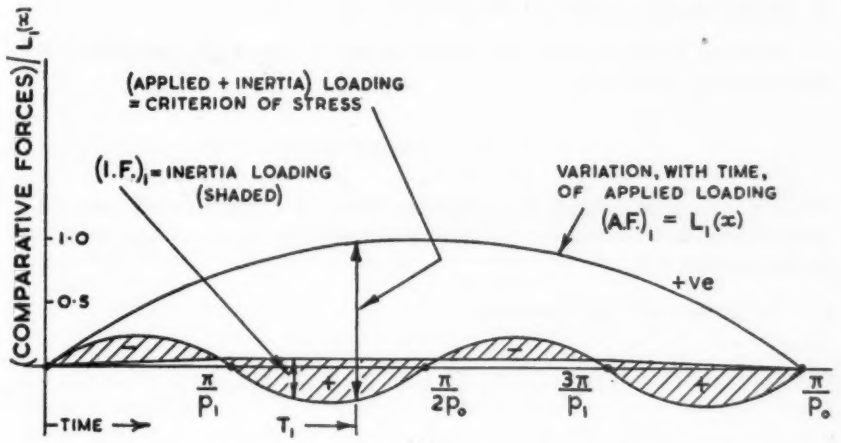


(*a*).

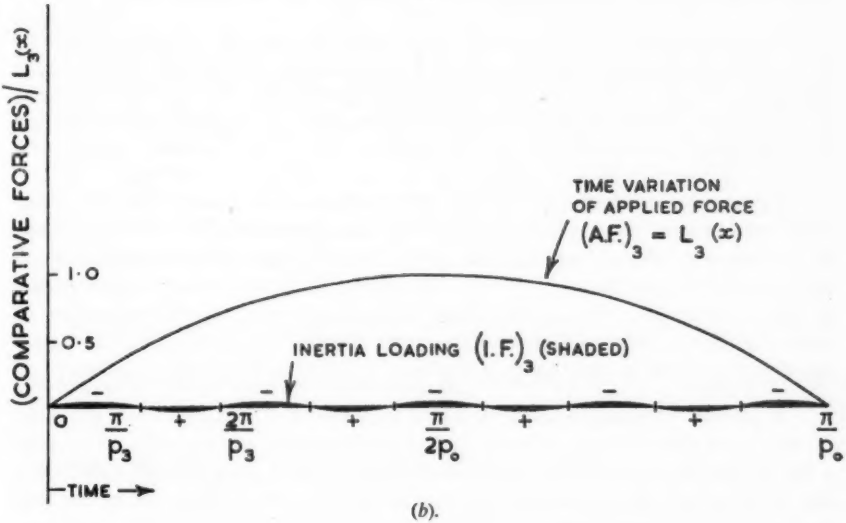


(*b*).

Fig. 5.

Showing how dynamic (*i.e.* inertia) effect is important only in first mode and its negligible value in the second mode.

(*a*) Time variation of applied and of inertia loading in first mode (both spatially distributed as $L_1(x)$ of Fig. 4(*b*)).

(*b*) Time variation of applied and of inertia loading in second mode (both spatially distributed as $L_3(x)$ of Fig. 4(*b*)).

## 7. SOME SHORT CUTS IN PRACTICAL PROBLEMS

In actual practice it may often be convenient to expand the time function $F(t)$ into a Fourier series giving

$$F(t)=\sum_{i=1}^{r} A_i \sin(i\pi t/T) \quad . \quad . \quad . \quad . \quad (12)$$

where $T$ is the total duration of the transient force, $i$ is a general symbol and $r$ is as small as possible consistent with the sum of $r$ terms being a fairly good representation of the function $F(t)$.

The integral in (6) then becomes

$$\int_0^t \cos p_n(t-t_1) \sum_{i=1}^{r} (i\pi/T) A_i \cos(i\pi t_1/T)\, dt_1 \quad . \quad . \quad . \quad (13)$$

which is easy to deal with analytically.

It is of interest to note a possible short cut in the process of representing $F(t)$ by a Fourier expansion, and the same short cut applies to the use of $F(t)$ in its unexpanded form. This consists of dividing the function $F(t)$ into two or more distinct parts as shown in Figs. 6 (*a*) and 6 (*b*) where the original curve is divided into two parts.

Figure 6 (*a*) shows the curve of $F(t)$ as a function of $t$, having a moderately even contour, apart from a sharp perturbation over the region $CD$. This curve can be divided into two components, one $F_1(t)$, which is everywhere smooth and has the same duration as the original $F(t)$, and another $F_2(t)$ which has a much smaller duration. It requires no mathematical proof to see that the representation of curves (*b*) by two separate Fourier series over different time intervals is a far easier task than representing curve (*a*) by a single series to the same degree of accuracy.

A parallel computational economy is achieved if $F_1(t)$ and $F_2(t)$ are used in their unexpanded form. For $F_1(t)$ is smooth enough not to excite more than a few of the graver modes of the system, while $F_2(t)$ is sharp enough to excite a few of the higher modes without affecting the graver modes. This will be the case particularly if the total impulse of $F_2(t)$ is zero, *i.e.* if the area under the curve $F_2(t)$ relative to the base line is zero.

*Note.* A most useful short cut is made by realising that it is never necessary in practice to compute the component normal loadings $L_1(x)$, $L_2(x)$, etc., for the purpose of estimating their inertia effects: it is only necessary to determine the *shape* of the corresponding normal modes of displacement. Thus it is not necessary to calculate the value of $L_n(x)$ before we can find the bending moments it produces

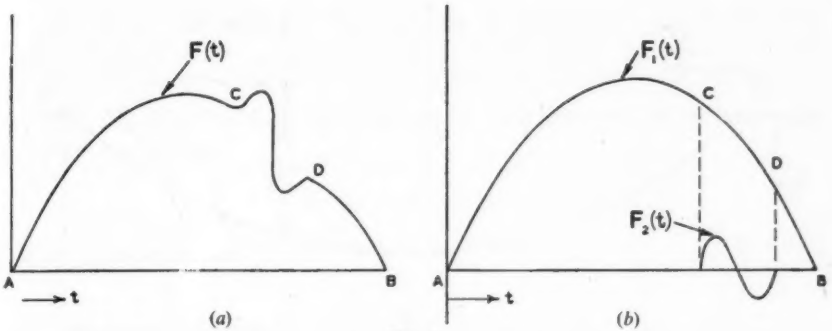


Fig. 6.

and hence, the bending moments of the corresponding inertia forces $(\text{I.F.})_n$. This follows from the fact that, *so long as the beam (or system) is constrained to deform in the $n^{th}$ mode*, the bending moments produced by the $n^{th}$ normal component loading of the applied load $P(x)$ are identical with those produced by the applied load itself.

Suppose for example, that the curve in Fig. 7 (which *must* be obtained either by calculation or from a resonance test) represents the shape of the first (or fundamental) normal mode of the beam $AB$ having a mass distribution $m(x)$. We require the bending moments produced in this mode by the first normal loading $L_1(x)$ without computing the value of $L_1(x)$ (which resulted in equation (10) in the numerical example above). All we have to do is to equate the strain energy in the beam to the work done by $Q$, *i.e.* $Qy_1/2$, from which $y_1$ (the displacement of $Q$) is determined, and hence the value of $y$, and so the bending moment, at all other sections.

In calculating the internal energy, moreover, it may be noted that it is far more accurate and convenient to compute the kinetic energy $\frac{p_1^2}{2}\int_0^l m(x)\,y^2 dx$ rather than the strain energy $\frac{E}{2}\int_0^l I\left(\frac{d^2y}{dx^2}\right)^2 dx$ to which it is equal.

## PART II

## 8. APPLICATION OF THE METHOD TO IRREGULAR SYSTEMS

The segregation of the inertia forces from the total resistance to the applied transient force, which is the basis of the above method, depends upon finding for each mode the Equivalent Static Force (E.S.F.) and expressing the Inertia Force

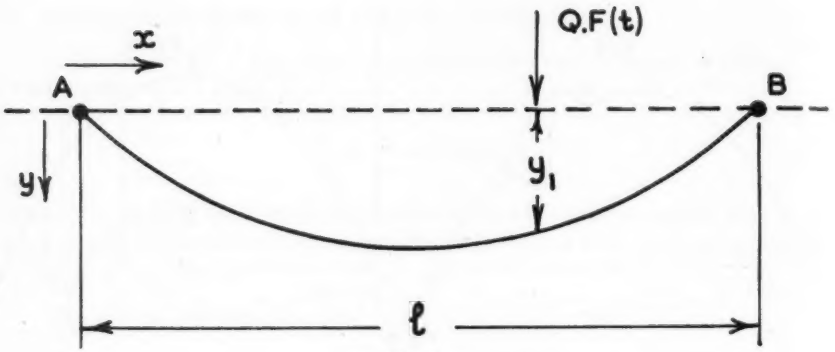


Fig. 7.

as the difference between the Applied Force and the Equivalent Static Force. The applied force is known, being part of the data of the problem, and the E.S.F. for each mode is expressible in terms of the frequency alone. However irregular the elastic system may be, its frequencies in the various modes, if not calculable, can always be found by experiment. It follows, therefore, that the inertia forces can be expressed as certain static forces in the various modes.

The difficulty with the irregular system is in translating the static forces in the various modes into displacements and stresses in the system, and the main source of that difficulty is that we cannot define the modes analytically, nor measure them experimentally. This point will be made clear by considering a practical example such as an aeroplane with a heavy gun mounted in the fuselage nose. Certain high frequency modes are excited in the structure adjacent to the gun mounting by the transient forces from the gun reaction. The frequencies of these modes can be found experimentally by applying a harmonically oscillating force along the gun barrel at gradually increasing frequencies and noting the resonance frequencies. The modes themselves cannot be found nor, therefore, the relation between the displacements in any mode and the static force at the gun necessary to produce them.

The engineer is not so much interested in displacements as in stresses and it is possible to relate the stresses in any mode directly to the static load. The procedure is as follows:—

At, and in the neighbourhood of, each resonance frequency, the amplitude at the point concerned—in this case at, and in the direction of, the gun barrel—is noted; the magnitude of the oscillating force and *the stresses at various relevant points in the surrounding structure are also noted.* The latter would be measured in practice by the use of a number of resistance strain gauges in conjunction with an oscillograph.

## DISPLACEMENTS OF A LINEAR ELASTIC SYSTEM

The purpose of measuring the amplitude at neighbouring frequencies is to obtain the shape of the resonance peak as accurately as possible so as to deduce from this the amount of damping present at the particular resonance frequency.

The differential equation for a damped system under forced vibration may be written in the form

$$m\ddot{z} + c\dot{z} + kz = F_o \sin \omega t$$

and the steady amplitude is

$$Z = \frac{F_o/k}{\sqrt{\left\{\left(1 - \frac{\omega^2}{\omega_n{}^2}\right)^2 + 4\left(\frac{c}{c_c}\frac{\omega}{\omega_n}\right)^2\right\}}}$$

where $k$ = the force per unit static displacement along $z$.

$\omega_n$ = resonance frequency for the $n^{th}$ mode.

$c_c$ = critical damping.

By taking two values of $z$ corresponding to two values of $\omega$ in the same resonance peak, $k$ can be eliminated and the value of $c/c_c$ obtained.

We have then, at resonance

$$Z_o = (F_o/k)/(2c/c_c)$$

from which $k$ may be found, since $c/c_c$ is now known as well as the oscillating force $F_o$.

Thus the relation between stresses and unit static displacement in any mode is established, enabling us to find in turn the stresses corresponding to the inertia forces in the various modes, and hence to apply the method given in Part I.

### REFERENCE

1. WILLIAMS, D., and JONES, R. P. N. (1948). Dynamic Loads in Aeroplanes Under Given Impulsive Loads with Particular Reference to Landing and Gust Loads on a Large Flying Boat. R. & M. 2221, 1948.

### NOTATION

$P(x)$ spatial distribution of applied load over the structure concerned at maximum value (when $F(t) = 1$).

| | |
|---|---|
| $F(t)$ | time variation of *magnitude* of $P(x)$, (whose curve of spatial distribution has a shape independent of time). $P(x) . F(t)$ is a maximum when $F(t)=1$. |
| $L_n(x)$ | $n^{th}$ normal loading component of $P(x)$, subject to the same time variation $F(t)$ as $P(x)$ itself. |
| $f_n(t)$ | time variation of inertia loading in $n^{th}$ mode (different for each mode). |
| $p_n$ | circular frequency of structural system in $n^{th}$ mode. |
| $p_o$ | circular frequency of harmonical force $Q \sin p_o t$ in the example. |
| $t_1$ | current time as distinct from a particular instant defined by $t$. |
| $(\text{E.S.F.})_n$ | Equivalent Static Force in the $n^{th}$ mode, denoting the steady static force (having the same distribution as $L_n(x)$) that produces the same *displacement* as that actually produced dynamically at any given instant in the $n^{th}$ mode. It is equal and opposite to the elastic resisting force. |
| $(\text{A.F.})_n$ | $L_n(x) . F(t)$. |
| $(\text{I.F.})_n$ | inertia loading in the $n^{th}$ mode having the same spatial distribution as $L_n(x)$ but its own time variation $f_n(t)$. |
| $\dot{F}(t)$ | $dF(t)/dt$. |
| $Q$ | spatial distribution $P(x)$ of applied load in numerical example. |
| $l$ | length of beam. |
| $i$ | general symbol denoting the $i^{th}$ Fourier component defining $F(t)$. |
| $T$ | total duration of transient force. |
| $m$ | mass. |
| $c$ | damping coefficient. |
| $c_c$ | critical damping coefficient. |
| $F_o$ | amplitude of harmonic force $F_o \sin \omega t$. |
| $k$ | elastic coefficient. |
| $\omega$ | circular frequency of forced vibration. |
| $\omega_n$ | resonance frequency of system in $n^{th}$ mode. |
| $I$ | moment of inertia. |
| $E$ | Young's modulus. |

# SKIN FRICTION IN THE LAMINAR BOUNDARY LAYER IN COMPRESSIBLE FLOW

by

A. D. YOUNG, M.A., A.F.R.Ae.S.

*(Department of Aerodynamics, College of Aeronautics, Cranfield)*

## SUMMARY

From an analysis of the work of Crocco and others, semi-empirical formulæ are derived for the skin friction on a flat plate at zero incidence with a laminar boundary layer. These formulæ are

$$c_f\sqrt{R_x}=0.664\,[0.45+0.55i\,(0)+0.09\,(\gamma-1)\,M_1^2\sigma^{\frac{1}{3}}]^{\frac{\omega-1}{2}}$$

for the general case of heat transfer, and

$$c_f\sqrt{R_x}=0.664\,[1+0.365\,(\gamma-1)\,M_1^2\sigma^{\frac{1}{3}}]^{\frac{\omega-1}{2}}$$

when there is no heat transfer.

The problem of heat transfer and the effect of radiation are discussed in the light of these formulæ. The second formula is then utilised in the development of an approximate method for solving the momentum equation of the boundary layer on a cylinder without heat transfer. The method indicates that with increase of Mach number there is a marked forward movement of separation from a flat plate in the presence of a constant adverse velocity gradient.

## NOTATION

The principal symbols used are listed below. Others are defined where they occur in the text.

Suffix 1 refers to quantities measured at outer edge of boundary layer, suffix "w" to quantities measured at the wall, suffix 0 to some standard condition, *e.g.* main stream at leading edge of plate, suffix "i" refers to incompressible flow.

---

Paper received November 1948.

[The Aeronautical Quarterly, Vol. 1, August 1949]

| | |
|---|---|
| $x$ | distance measured along surface. |
| $y$ | distance measured normal to surface. |
| $u$ | velocity component in $x$ direction. |
| $v$ | velocity component in $y$ direction. |
| $p$ | pressure. |
| $L$ | standard length (*e.g.* length of plate). |
| $M$ | Mach number. |
| $T$ | temperature (absolute). |
| $J$ | mechanical equivalent of heat. |
| $I$ | enthalpy ($=Jc_pT$, for a perfect gas with constant specific heats). |
| $c_p$ | specific heat at constant pressure. |
| $c_v$ | specific heat at constant volume. |
| $\gamma$ | $c_p/c_v$. |
| $\tau$ | viscous stress. |
| $\rho$ | density. |
| $\mu$ | coefficient of viscosity. |
| $\nu$ | $\mu/\rho$. |
| $\xi$ | constant $\times\, y/\sqrt{(2x)}$. |
| $k$ | coefficient of heat conduction. |
| $\sigma$ | Prandtl number $=\mu c_p/k$. |
| $\omega$ | defined by $\mu \propto T^{\omega}$. |
| $c_f$ | $2\tau_w/\rho_1 u_1^2$. |
| $R$ | $u_0 L/\nu_0$. |
| $R_x$ | $u_1 x/\nu_1$. |
| $R_L$ | $u_1 L/\nu_1$. |
| $i$ | $I/I_1$. |
| $j$ | $I/u_1^2$. |
| $\eta$ | $u/u_1$. |
| $r$ | $\rho/\rho_1$. |
| $m$ | $\mu/\mu_1$. |
| $f(u)$ | function defined in equation (6). |
| $f(M_0, \omega, \sigma)$ | function defined in equation (48). |

| | |
|---|---|
| $g(M_0, \omega, \sigma)$ | function defined in equation (51). |
| $F(\eta)$ | function defined in equation (9). |
| $G(\eta)$ | function defined in equation (17). |
| $Q$ | rate of transfer of heat from surface of unit breadth and length $L$ to gas. |
| $q$ | local rate of heat transfer per unit area. |
| $S_F$ | total frictional force on surface of unit breadth and length $L$. |
| $C_B$ | Stefan-Boltzmann's radiation constant × emissivity of surface. |
| $\theta$ | momentum thickness $= \int_0^\infty \frac{\rho u}{\rho_1 u_1}\left(1 - \frac{u}{u_1}\right) dy.$ |
| $\delta^{**}$ | displacement thickness $= \int_0^\infty \left(1 - \frac{\rho u}{\rho_1 u_1}\right) dy.$ |
| $H$ | $\delta^{**}/\theta$. |
| $Y$ | $\int_0^y \frac{\mu_0 dy}{\mu}$. |
| $\delta_1^*$ | the value of $Y$ defining the outer edge of the boundary layer. |
| $\rho^*$ | $\rho/\rho_0$. |
| $\mu^*$ | $\mu/\mu_0$. |
| $\theta^*$ | $\theta/L$. |
| $u^*$ | $u/u_0$. |
| $x^*$ | $x/L$. |
| $\Lambda$ | $u_1'\delta_1^{*2}\rho_1 \frac{\mu_w}{\mu_0^2}$. |

## 1. INTRODUCTION

The general analysis of the flow in the laminar boundary layer at high speeds is of formidable complexity. This complexity derives from the variation of viscosity, heat conductivity and density with temperature and the consequent inter-dependence of the equations of motion and energy. The simplest problem, namely uniform flow past a flat plate at zero incidence, has naturally attracted most attention; nevertheless results for particular cases have only been evaluated after long and laborious calculations. We are indebted for a store of such results to the work of Busemann[1], Kármán and Tsien[2], Hantzsche and Wendt[3], Emmons and Brainerd[4], Cope and Hartree[5], and Crocco[6]. The work of the latter is particularly important since, in addition to results for particular cases, it reveals results of a general character. The more general problem of the boundary layer on

a cylinder is still in large measure unsolved. Valuable pioneer work on lines analogous to Howarth's series solution for incompressible flow[7] has been begun by Cope and Hartree, and Howarth[8] has similarly developed solutions for the case when $\sigma = 1.0$, and $\omega = 1.0$. In addition, approximate methods have been developed by Frankl[9], Oswatitsch and Wieghardt[10], Young and Winterbottom[11], Illingworth[12], and Howarth[8], in which solutions are obtained of the momentum and energy equations on lines analogous to Pohlhausen's method[13], or in which other assumptions or approximations suggested by incompressible flow theory are made.

In the following a general semi-empirical formula is developed for the skin friction on a flat plate at zero incidence, both with and without heat transfer in a uniform flow of a perfect gas with constant specific heats. This formula is derived from an approximate solution of Crocco's integral equation for the viscous stress. The form of this solution is retained but the constants are adjusted to give the best overall agreement with the available calculated results for particular cases. The problem of heat transfer and the effect of radiation on the temperature measured by a thermometer are discussed briefly in the light of this formula.

The formula is then applied to the development of an approximate method for solving the momentum equation of the boundary layer on a cylinder with zero heat transfer. The accuracy of the method cannot yet be gauged, as there are no accurate results available with which to compare it. It has two features to commend it; firstly, it gives the correct result for the case of zero external pressure gradient; secondly, it is relatively simple and quick to apply, the main operation in any given case being a simple integration.

The method has been applied to estimate the distance to separate from a flat plate in the presence of a constant negative velocity gradient when $\sigma = 1.0$, and $\omega = 1.0$. This is the case considered by Howarth[8] by a method closely analogous to Pohlhausen's method. It is doubtful whether either method can be relied on to give the separation distance accurately, and their results differ considerably for high Mach numbers, but both methods agree in predicting a rapid forward movement of separation with increase of Mach number at the leading edge for constant ratio of (velocity fall per unit length of plate) to (initial velocity).

## 2. SKIN FRICTION ON A FLAT PLATE AT ZERO INCIDENCE

### 2.1. *Boundary layer equations*

The equations of motion for the boundary layer are

$$\left.\begin{aligned} \rho u \frac{\partial u}{\partial x} + \rho v \frac{\partial u}{\partial y} &= \frac{\partial}{\partial y}\left(\mu \frac{\partial u}{\partial y}\right), \\ \frac{\partial p}{\partial y} &= 0. \end{aligned}\right\} \quad . \quad . \quad . \quad . \quad (1)$$

The equation of continuity is

$$\frac{\partial}{\partial x}(\rho u)+\frac{\partial}{\partial y}(\rho v)=0, \quad . \quad . \quad . \quad . \quad . \quad . \quad (2)$$

and the equation of energy is

$$\rho u\frac{\partial I}{\partial x}+\rho v\frac{\partial I}{\partial y}=\frac{1}{\sigma}\frac{\partial}{\partial y}\left(\mu\frac{\partial I}{\partial y}\right)+\mu\left(\frac{\partial u}{\partial y}\right)^2, \quad . \quad . \quad (3)$$

when $I \equiv Jc_pT$ (enthalpy), and $\sigma$ is the Prandtl number $=\mu c_p/k$ and is assumed constant.

The equation of state for a perfect gas is

$$p=\rho\bar{R}T/\bar{m}, \quad . \quad . \quad . \quad . \quad . \quad . \quad (4)$$

where $\bar{R}$ is the gas constant and $\bar{m}$ is the molecular weight of the gas. Since $p$ is constant for the flat plate at zero incidence, $\rho=\rho(I)$.

The viscosity coefficient $\mu$ is a function of $T$ only, the relation being given by Sutherland's formula

$$\mu \propto \frac{T^{1.5}}{T+c}, \text{ where } c \text{ is a constant and is equal to } 110°\text{K, for air.}$$

It is convenient to approximate to this relation by writing

$$\mu \propto T^{\omega}, \quad . \quad . \quad . \quad . \quad . \quad . \quad (5)$$

where $\omega$ varies according to the range of $T$ in which we are interested, but can be taken equal to 8/9 for $T$ between 75°K and 300°K[14].

## 2.2. *Crocco's Transformation*[6]

The case of the flat plate at zero incidence is the only one which permits the reduction of the boundary layer equations to ordinary equations in terms of a single independent variable. This variable is of the form $\xi=\text{constant}\times y/\sqrt{(2x)}$. In this case we can write $I=I(u)$, $\rho=\rho(u)$, $\mu=\mu(u)$ and

$$\tau=\mu\left(\frac{\partial u}{\partial y}\right)=\mu\left(\frac{du}{d\xi}\right)\frac{\text{constant}}{\sqrt{(2x)}}=\frac{f(u)}{\sqrt{(2x)}}, \text{ say.} \quad . \quad . \quad . \quad (6)$$

If we transform from $\xi$ to $u$ as independent variable, the equations (1), (2) and (3)

reduce to two equations in $f$ and $I$, namely

$$ff'' + u\rho\mu = 0, \quad . \quad . \quad . \quad . \quad . \quad . \quad (7)$$

$$(I'' + \sigma) f + (1 - \sigma) I' f' = 0, \quad . \quad . \quad . \quad . \quad . \quad (8)$$

where dashes denote differentiation with respect to $u$.

These equations can be put into a non-dimensional form by writing

$$\frac{u}{u_1} = \eta, \ \frac{I}{I_1} = i, \ \frac{\rho}{\rho_1} = r, \ \frac{\mu}{\mu_1} = m, \ F(\eta) = \sqrt{\left(\frac{2}{\rho_1 \mu_1 u_1^3}\right)} f(u), \quad . \quad (9)$$

when suffix 1 refers to quantities in the main stream.

Equations (7) and (8) then become

$$FF'' + 2\eta r m = 0, \quad . \quad . \quad . \quad . \quad . \quad (10)$$

$$(i'' + \sigma u_1^2 / I_1) F + (1 - \sigma) i' F' = 0, \quad . \quad . \quad . \quad . \quad (11)$$

and we note that $u_1^2 / I_1 = (\gamma - 1) M_1^2$; dashes now indicate differentiation with respect to $\eta$.

The boundary conditions are

$$\eta = 0, \ F' = 0, \ i = I_w / I_1;$$

$$\eta = 1, \ F = 0, \ i = 1.$$

Suffix " w " denotes quantities measured at the wall.

The equation of state (4) gives

$$r = \frac{\rho}{\rho_1} = \frac{T_1}{T} = \frac{I_1}{I} = \frac{1}{i}, \quad . \quad . \quad . \quad . \quad . \quad (12)$$

and the viscosity—temperature relation (5) becomes

$$m = i^{\omega}. \quad . \quad . \quad . \quad . \quad . \quad . \quad (13)$$

Using (12) and (13), equation (10) can be written

$$FF'' + 2\eta i^{-(1-\omega)} = 0. \quad . \quad . \quad . \quad . \quad . \quad (14)$$

From (6) and (9) it is easy to deduce that

$$c_f \sqrt{R_x} = F(0) \quad . \quad . \quad . \quad . \quad . \quad . \quad (15)$$

where $c_f$ is the local skin friction coefficient ($=2\tau_w/\rho_1 u_1^2$) at a point distant $x$ from the leading edge, and $R_x = u_1 x/\nu_1$.

Once $F(\eta)$ is determined, the relation between $y$ and $u$ is given by (6) and hence

$$y = \int_0^u \frac{\mu du}{\tau(x, u)},$$

which reduces to

$$\frac{u_1 y}{\nu_1} = 2\sqrt{R_x} \int_0^\eta \frac{m}{F(\eta)} d\eta. \quad . \quad . \quad . \quad . \quad . \quad (16)$$

## 2.3. *Hantzsche and Wendt's Transformation*[3]

Hantzsche and Wendt arrived at different forms of these equations by using different non-dimensional expressions involving $I$ and $f(u)$. Thus, they wrote

$$j = I/u_1^2, \text{ and } G(\eta) = \sqrt{\left(\frac{2}{\mu_w \rho_w u_1^3}\right)} . f(u). \quad . \quad . \quad . \quad (17)$$

and their resulting equations which correspond to (14) and (11) were

$$GG'' + 2\eta (j_w/j)^{1-\omega} = 0, \quad . \quad . \quad . \quad . \quad (18)$$

and

$$G(j'' + \sigma) + (1-\sigma) G' j' = 0. \quad . \quad . \quad . \quad . \quad (19)$$

In this case the skin friction coefficient is given by

$$c_f \sqrt{R_x} = G(0) (j_1/j_w)^{\frac{1-\omega}{2}} = G(0) (T_1/T_w)^{\frac{1-\omega}{2}} \quad . \quad . \quad . \quad (20)$$

## 2.4. *Some important results of Crocco's analysis*

It will immediately be apparent from the form of equations (14) and (11) (or from equations (18) and (19)) that considerable simplifications result when $\rho\mu =$ constant and hence $\omega = 1.0$, or when $\sigma = 1.0$.

Thus, *when* $\sigma = 1.0$, equation (11) reduces to

$$i'' + u_1^2/I_1 = 0, \quad . \quad . \quad . \quad . \quad . \quad (21)$$

and hence $i$ is a quadratic function of $\eta$, independent of $F$; taking account of the boundary conditions this function may be written

$$\left.\begin{aligned} i &= 1 - i'(0)(1-\eta) + \frac{u_1^2}{2I_1}(1-\eta^2), \\ \text{or} \qquad i &= i(0) + \left[1 - i(0) + \frac{u_1^2}{2I_1}\right]\eta - \frac{u_1^2}{2I_1}\eta^2. \end{aligned}\right\} \quad . \quad . \quad . \quad (22)$$

Having $i$ as a function of $u$, equation (14) for $F$ takes the form

$$FF'' + h(\eta) = 0$$

where $h(\eta)$ is known. For details of an iterative process that can be used to solve this equation for $F$ *see* Ref. 6.

*When* $\rho\mu$ = constant *or* $\omega = 1.0$, equation (14) simplifies to

$$FF'' + 2\eta = 0, \quad . \quad . \quad . \quad . \quad . \quad . \quad . \quad (23)$$

which can be transformed to the Blasius equation for incompressible flow, namely,

$$\frac{d^3\zeta}{d\xi^3} + \zeta\frac{d^2\zeta}{d\xi^2} = 0,$$

by writing $F = \frac{1}{2}\frac{d^2\zeta}{d\xi^2}$, $\eta = \frac{1}{2}\frac{d\zeta}{d\xi}$.

The relation between $\xi$ and $y_1$, the lateral ordinate in incompressible flow, is

$$\xi = \tfrac{1}{2}\sqrt{\left(\frac{u_1}{\nu_1}\right)}\left(\frac{y_1}{\sqrt{x}}\right).$$

From equation (16), the lateral ordinate in compressible flow corresponding to a given value of $\eta$ is

$$y = \frac{2x}{\sqrt{R_x}}\int_0^{\eta}\frac{m\,d\eta}{F(\eta)} = \frac{2x}{\sqrt{R_x}}\int_0^{\xi} m\,d\xi = \int_0^{y_1} m\,dy_1$$

$$= \int_0^{y_1}\frac{\mu}{\mu_1}\,dy_1 \qquad = \int_0^{y_1}\frac{i}{i_1}\,dy_1. \quad . \quad . \quad . \quad . \quad . \quad . \quad (24)$$

Hence for this case all solutions are simple transformations of the incompressible flow solution, the relation between corresponding values of $y$ for given values of $u$ (or $\eta$) being given by equation (24).

We note immediately that since $\eta = 0$ when $\xi = 0$, $F(0)$ is the same for compressible as for incompressible flow and *hence in all cases when* $\rho\mu$ = constant

(*or* $\omega = 1.0$)

$$c_f \sqrt{R_x} = F(0) = 0.664. \quad . \quad . \quad . \quad . \quad . \quad (25)$$

In the general case, when neither $\omega$ nor $\sigma$ is necessarily unity, let us suppose we have solved for $F$ as a function of $\eta$. Then equation (11) which is linear in $i$ can be integrated twice to give

$$\left.\begin{aligned} i(\eta) &= i(0) + i'(0)\, A(\eta, \sigma) - \sigma (u_1^2/I_1)\, B(\eta, \sigma), \\ \text{where} \quad A(\eta, \sigma) &= \int_0^{\eta} \left[\frac{F(\eta_1)}{F(0)}\right]^{\sigma-1} d\eta_1, \\ \text{and} \quad B(\eta, \sigma) &= \int_0^{\eta} \left[\frac{F(\eta_1)}{F(0)}\right]^{\sigma-1} \left\{ \int_0^{\eta_1} \left[\frac{F(\eta_2)}{F(0)}\right]^{1-\sigma} d\eta_2 \right\} d\eta_1. \end{aligned}\right\} \quad . \quad . \quad (26)$$

Alternatively, taking account of the fact that $i(1) = 1$, we have

$$\left.\begin{aligned} i(\eta) &= 1 - i'(0)\, C(\eta, \sigma) + \sigma (u_1^2/I_1)\, D(\eta, \sigma), \\ \text{where} \quad C(\eta, \sigma) &= \int_{\eta}^{1} \left[\frac{F(\eta_1)}{F(0)}\right]^{\sigma-1} d\eta_1, \\ \text{and} \quad D(\eta, \sigma) &= \int_{\eta}^{1} \left[\frac{F(\eta_1)}{F(0)}\right]^{\sigma-1} \left\{ \int_0^{\eta_1} \left[\frac{F(\eta_2)}{F(0)}\right]^{1-\sigma} d\eta_2 \right\} d\eta_1. \end{aligned}\right\} \quad . \quad . \quad (27)$$

Hence, for the case of zero heat transfer when $i'(0) = 0$

$$\left.\begin{aligned} \frac{I(\eta) - I(1)}{u_1^2/2} &= 2\sigma D(\eta, \sigma), \\ \text{and in particular} \quad \frac{I(0) - I(1)}{u_1^2/2} &= 2\sigma D(0, \sigma). \end{aligned}\right\} \quad . \quad . \quad . \quad . \quad (28)$$

Since $D(0, \sigma)$ does not involve $M_1$, it will be independent of Mach number for all cases where $F(\eta)$ is independent of Mach number, *i.e.* for all cases where $\rho\mu = \text{constant}$ (or $\omega = 1.0$). Pohlhausen's solution[15] for incompressible flow gave to a very close order of accuracy

$$\frac{I(0) - I(1)}{u_1^2/2} = \sigma^{\frac{1}{2}},$$

hence

$$2\sigma D(0, \sigma) = \sigma^{\frac{1}{2}},$$

and therefore for all cases where $\rho\mu = \text{constant}$,

$$\frac{T_w}{T_1} = 1 + \frac{(\gamma-1)}{2} M_1^2 \sigma^{\frac{1}{2}}. \quad . \quad . \quad . \quad . \quad . \quad (29)$$

However, by a laborious trial and error method Crocco[6] integrated equations (11) and (14) step by step for the cases $\sigma = 0.725$, a range of Mach numbers up to 5.0 and values of $\omega$ of 1.25, 0.75 and 0.5. In every case the results showed the functions $A$, $B$, $C$ and $D$ to be practically independent of the particular value of $\omega$ assumed, and hence independent of the function $F(\eta)$ within the range of values of $\omega$ considered. Crocco suggested that the reason for this lay in the fact that while the variation of $F(\eta)$ with $\omega$ may be considerable, it occurs in the integrals from which $A$, $B$, $C$ and $D$ are derived in the form $\left[\frac{F(\eta)}{F(0)}\right]^{1-\sigma}$ or $\left[\frac{F(\eta)}{F(0)}\right]^{\sigma-1}$. The ratio $F(\eta)/F(0)$ must in every case be unity when $\eta = 0$, and be zero when $\eta = 1.0$, and hence its possible variation with $\omega$ is limited. Further, as long as $\sigma$ is not far off unity, the exponents $(1-\sigma)$ or $(\sigma-1)$ are small and reduce still further the sensitivity of the expressions $A$, $B$, $C$ and $D$ to variations in $\omega$. The final result is therefore that in general the variation of enthalpy with velocity is practically independent of the viscosity—temperature relation for values of $\sigma$ not very different from unity, and is given by equations (26) or (27) with the functions $A$, $B$, $C$ and $D$ calculated for the case $\omega = 1.0$, when $F(\eta)$ is given immediately by the Blasius incompressible flow solution. In particular, when there is zero heat transfer, equation (29) for the wall temperature is of general validity, a fact that is confirmed by the cases calculated by Brainerd and Emmons[4].

Since $i(\eta)$ can now be regarded as independent of $F(\eta)$ in general, and is readily determined from the case $\omega = 1.0$, the solution of the main equations (10) and (11) reduces to the solution of the equation

$$FF'' + h(\eta) = 0,$$

where $h(\eta)$ is known. This enabled Crocco to develop a more rapid and more accurate process of solution than the first process he had used. For further details *see* Ref. 6.

## 2.5. *Skin friction distribution. Deduction from Hantzsche and Wendt's results for case of zero heat transfer*

Hantzsche and Wendt's calculations[3] for the case of zero heat transfer showed the interesting result that the quantity $G(0)$ was only a slightly varying function of $\omega$ and $M_1$ for $\sigma = 1.0$, and was independent of $\sigma$ and $M_1$ when $\omega = 1.0$. In general, therefore, we may expect $G(0)$ to vary little with $\sigma$, $\omega$ and $M_1$. The importance of this may be seen from equation (20) which with equation (29) gives us

$$c_f \sqrt{R_x} = G(0) \Big/ \left[1 + \frac{(\gamma-1)}{2} M_1^2 \sigma^{\frac{1}{3}}\right]^{\frac{1-\omega}{2}}. \quad . \quad . \quad . \quad (30)$$

A reasonable approximation to $G(0)$, reproducing its small variation with $\omega$, $\sigma$ and $M_1$ should then give us a reliable formula for $c_f \sqrt{R_x}$, for which the major variation with $\omega$, $\sigma$ and $M_1$ is described by the denominator of (30). In Fig. 1, $G(0)$ is shown as a function of $M_1$ for various values of $\omega$, for the case $\sigma = 1.0$, and this can be represented fairly closely by

$$G(0) \approx 0.664 \left[\frac{1 + \frac{\gamma-1}{2} M_1^2}{1 + 0.3(\gamma-1) M_1^2}\right]^{\frac{1-\omega}{2}}.$$

This suggests that in general

$$G(0) \approx 0.664 \left[\frac{1 + \frac{\gamma-1}{2} M_1^2 \sigma^{\frac{1}{3}}}{1 + 0.3(\gamma-1) M_1^2 \sigma^{\frac{1}{3}}}\right]^{\frac{1-\omega}{2}},$$

and hence for the case of zero heat transfer we may expect from (30) that

$$\frac{c_f \sqrt{R_x}}{0.664} = \frac{F(0)}{F(0)_{\omega=1}} \approx [1 + 0.3(\gamma-1) M_1^2 \sigma^{\frac{1}{3}}]^{-\frac{1-\omega}{2}} \quad . \quad . \quad (31)$$

## 2.6. *Skin friction distribution with or without heat transfer. Deduction from approximate solution of integral equation for F*

From equation (14) and the boundary conditions for $F$ it follows that

$$F = \int_{\eta_1}^{1} \left[\int_0^{\eta_1} \frac{2\eta i^{\omega-1}}{F} d\eta\right] d\eta_1. \quad . \quad . \quad . \quad . \quad . \quad (32)$$

From a survey of Crocco's results for $F$ it appears that in all cases a very close

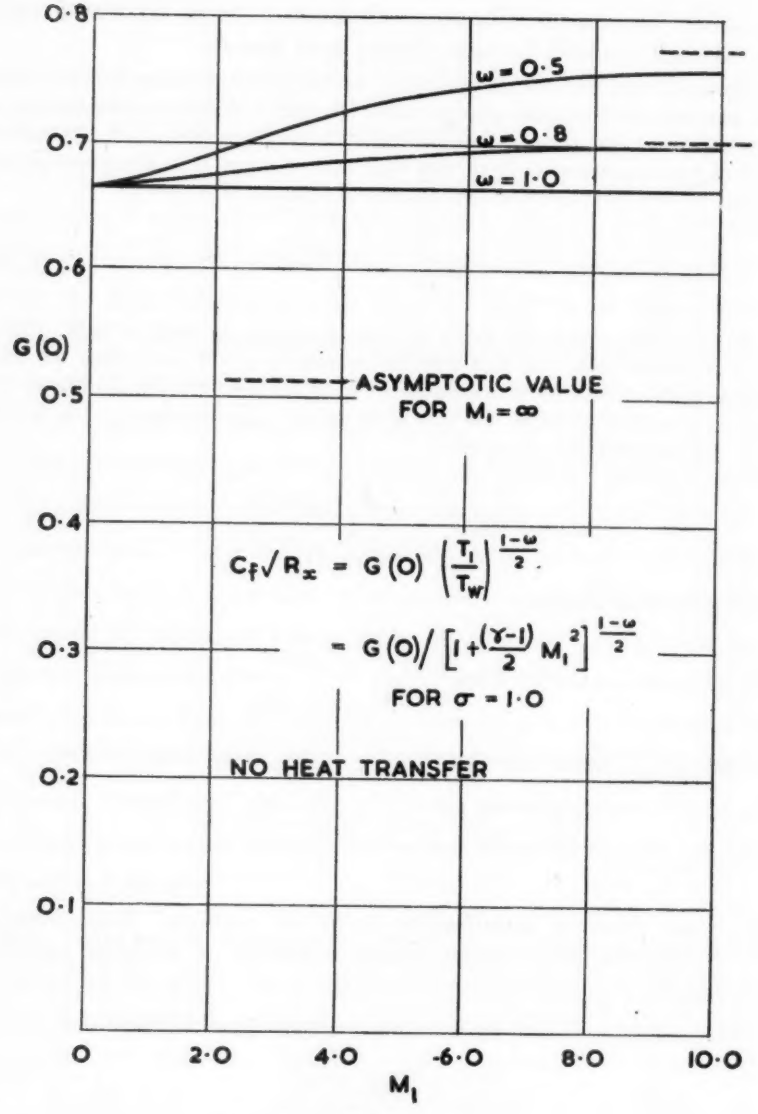


Fig. 1.

Skin friction of flat plate at zero incidence (no heat transfer).
The function $G(0)$ according to calculations of Hantzsche and Wendt ($\sigma = 1.0$).

fit to $F$ is given by

$$F \approx F(0)(1-\eta^2)^{\frac{1}{2}}.$$

Hence, from (32) we may expect to get an even closer fit from the relation

$$F \approx \int_{\eta_1}^{1} \left[ \int_0^{\eta_1} \frac{2\eta i^{\omega-1}}{F(0)(1-\eta^2)^{\frac{1}{2}}} \, d\eta \right] d\eta_1.$$

In particular,

$$F(0)^2 \approx \int_0^1 \left[ \int_0^{\eta_1} \frac{2\eta i^{\omega-1}}{(1-\eta^2)^{\frac{1}{2}}} \, d\eta \right] d\eta_1. \quad . \quad . \quad . \quad . \quad (33)$$

We have $i$ as a function of $\eta$ and $\sigma$ given by (26) or (27) so that in theory we can determine $F(0)^2$ from (33) in any given case by integration (which must in general be numerical), and hence from (15) we can obtain the skin friction coefficient. We are interested, however, in obtaining a general explicit formula for $F(0)$ in terms of $i(0)$ (or $T_w/T_1$), $M_1$, $\sigma$ and $\omega$. Analytic integration of (33) appears to be impossible in general; the process adopted, therefore, has been to develop a crude approximate solution of (33) to suggest the form of the required formula for $F(0)$; the constants in this formula have then been adjusted to give the best fit with the numerical results of Crocco and other workers.

Consider the case when $\sigma = 1.0$. Then we can write

$$i = A_1 + A_2\eta + A_3\eta^2,$$

where $A_1 = i(0)$, $A_2 = 1 - i(0) + u_1^2/2I_1$, $A_3 = -u_1^2/2I_1$.

Write $\eta = \sin\chi$, then (33) can be written

$$F(0)^2 = \int_0^{\frac{\pi}{2}} \left[ \int_0^{\chi_1} 2\sin\chi\,(A_1 + A_2\sin\chi + A_3\sin^2\chi)^{\omega-1} \, d\chi \right] d\chi_1.$$

Let $A_4 = 1 + i(0) + u_1^2/2I_1$, then $A_4 > A_1 + A_2\sin\chi + A_3\sin^2\chi$.

Hence, we can write

$$F(0)^2 = A_4^{\omega-1} \int_0^{\frac{\pi}{2}} \left[ \int_0^{\chi_1} 2\sin\chi \left[ 1 + (\omega-1)\left( \frac{A_2}{A_4}\sin\chi + \frac{A_3}{A_4}\sin^2\chi - \frac{A_4 - A_1}{A_4} \right) + \ldots \right] \right] d\chi_1,$$

$$= A_4^{\omega-1} \left\{ 2 - \frac{\pi}{2} + (\omega-1)\left[ \left( \frac{A_1 - A_4}{A_4} \right)\left( 2 - \frac{\pi}{2} \right) + \frac{A_2}{A_4}\left( \frac{\pi}{2} - \frac{4}{3} \right) + \right. \right.$$

$$\left. \left. + \frac{A_3}{2A_4}\left( \frac{8}{3} - \frac{3\pi}{4} \right) \right] + \text{terms in } (\omega-1)^2 \right\}. \quad (34)$$

This leads to the result that when $\omega = 1.0$,

$$F(0)^2 = 2 - \frac{\pi}{2},$$

and therefore $F(0) = 0.655$ (compare the accurate value of 0.664).

Write equation (34) in the form

$$\frac{F(0)}{F(0)_{\omega=1}} = A_4^{\frac{\omega-1}{2}} \left\{ 1 + (\omega - 1) \left[ \frac{A_1 - A_4}{A_4} + \frac{A_2}{A_4} \frac{(3\pi - 8)}{(12 - 3\pi)} + \right. \right.$$
$$\left. \left. + \frac{A_3}{12 A_4} \frac{(32 - 9\pi)}{(4 - \pi)} \right] + \text{terms in } (\omega - 1)^2 \right\}^{\frac{1}{2}}$$

Then assuming $\omega$ is not very far from unity (as will be the case in practice), the terms in $(\omega - 1)^2$ can be allowed for to some extent by approximating to the right hand side with

$$\frac{F(0)}{F(0)_{\omega=1}} = \left\{ A_4 + (A_1 - A_4) + A_2 \left( \frac{3\pi - 8}{12 - 3\pi} \right) + \frac{A_3}{12} \frac{(32 - 9\pi)}{(4 - \pi)} \right\}^{\frac{\omega-1}{2}}$$
$$= \left\{ \frac{3\pi - 8}{12 - 3\pi} + i(0) \left[ \frac{20 - 6\pi}{12 - 3\pi} \right] + \frac{u_1^2}{2I_1} \left[ \frac{21\pi - 64}{12(4 - \pi)} \right] \right\}^{\frac{\omega-1}{2}}$$
$$= [0.553 + 0.447\, i(0) + 0.096\, u_1^2/I_1]^{\frac{\omega-1}{2}} \quad . \quad . \quad . \quad . \quad . \quad (35)$$

Even before any attempt is made to modify the constants in this formula to improve agreement with calculated results we may note that it gives good agreement with formula (31) for the case of zero heat transfer and $\sigma = 1.0$. Thus, in this case, from (29),

$$i(0) = 1 + \frac{(\gamma - 1)}{2} M_1^2 = 1 + u_1^2/2I_1,$$

and hence (35) becomes

$$\frac{F(0)}{F(0)_{\omega=1}} = [1 + 0.32\, u_1^2/I_1]^{\frac{\omega-1}{2}} = [1 + 0.32(\gamma - 1) M_1^2]^{\frac{\omega-1}{2}}.$$

This comparison indicates that any modification to (35) should retain the following features:—

(*i*) The sum of the constant term and the coefficient of $i(0)$ should be unity.

(*ii*) Half the coefficient of $i(0)$ plus the coefficient of $u_1^2/I_1$ should be approximately equal to 0.3.

The comparison also indicates that to take account of values of $\sigma$ other than unity the coefficient of $u_1^2/I_1$ should include the term $\sigma^{\frac{1}{2}}$.

Formula (35) with this last modification was in fact found to give results in surprisingly close agreement with the calculations of Refs. 2 to 6, bearing in mind the approximate nature of the analysis. The closest overall agreement was found, however, with the formula

$$\frac{F(0)}{F(0)_{\omega=1}} = [0.45 + 0.55\, i\,(0) + 0.09\,(\gamma-1)\,M_1^2\sigma^{\frac{1}{2}}]^{\frac{\omega-1}{2}}.$$

Using the correct basic value of $F(0)_{\omega=1} = 0.664$, this can be written

$$c_f\sqrt{R_x} = 0.664\,[0.45 + 0.55 i\,(0) + 0.09\,(\gamma-1)\,M_1^2\sigma^{\frac{1}{2}}]^{\frac{\omega-1}{2}}. \quad . \quad (36)$$

For the case of zero heat transfer this reduces to

$$c_f\sqrt{R_x} = 0.664\,[1 + 0.365\,(\gamma-1)\,M_1^2\sigma^{\frac{1}{2}}]^{\frac{\omega-1}{2}} \quad . \quad . \quad . \quad . \quad (37)$$

Table I compares the results given by equation (36) and Crocco's calculations, and it will be seen that in every case the agreement is within one per cent., which is within the accuracy of Crocco's calculations. In Table II Crocco's results for zero heat transfer are compared with the results given by equation (37), and the agreement will be seen to be equally good. Finally, in Fig. 2 some of the results of Refs. 2, 4 and 5 are compared with equation (37) for the case of zero heat transfer, and in every case close agreement is found. One can conclude that the formulæ (36) and (37) are reliable to within about one per cent. for values of the Mach number up to 10, and for values of $\omega$ and $\sigma$ likely to be of practical interest when air is the working fluid.†

## 3. HEAT TRANSFER AND RADIATION—FLAT PLATE AT ZERO INCIDENCE

### *3.1. Heat transfer*

If $Q$ is the total heat transferred per unit time from a surface of unit breadth and of length $L$, say, $q$ is the local rate of heat transfer per unit area and $S_F$ is the total frictional force on the surface, then it readily follows from Crocco's analysis that for $\sigma$ near unity

$$\frac{Q}{S_F} = \frac{q}{\tau_\omega} = \frac{Jc_p}{\sigma^{2/3}}\left[\frac{T_w - T_{th}}{u_1}\right], \quad . \quad . \quad . \quad . \quad (38)$$

where $T_{th}$ is the temperature measured by a thermometer, *i.e.* $T_{th} = T_w$ for zero

† The coefficient of $(\gamma-1)\,M_1^2\sigma^{\frac{1}{2}}$ in equation (37) is somewhat greater than that suggested by equation (31) based on Hantzsche and Wendt's results. However, the complexity of the computations involved leaves it likely that small systematic errors may have been present in the latter's calculations.

## TABLE I

Comparison of Crocco's calculated values of skin friction on a flat plate with values given by equation (36) ($\sigma = 0.725$).

| $M_1$ | $\omega$ | $i(0)$ | $\frac{c_f\sqrt{R_x}}{(c_f\sqrt{R_x})_{\omega=1}}$ † (Crocco) | $\frac{c_f\sqrt{R_x}}{0.664}$ (Equation (36)) |
|---|---|---|---|---|
| 1 | 1.25 | 0.25 | 0.940 | 0.942 |
| 2 | 1.25 | 0.25 | 0.957 | 0.960 |
| 5 | 1.25 | 0.25 | 1.040 | 1.039 |
| 1 | 1.25 | 1.0 | 1.006 | 1.004 |
| 2 | 1.25 | 1.0 | 1.016 | 1.015 |
| 5 | 1.25 | 1.0 | 1.076 | 1.074 |
| 1 | 1.25 | 2.0 | 1.056 | 1.059 |
| 2 | 1.25 | 2.0 | 1.066 | 1.066 |
| 5 | 1.25 | 2.0 | 1.111 | 1.111 |
| 1 | 0.75 | 0.25 | 1.070 | 1.062 |
| 2 | 0.75 | 0.25 | 1.049 | 1.041 |
| 5 | 0.75 | 0.25 | 0.960 | 0.963 |
| 1 | 0.75 | 1.0 | 0.996 | 0.996 |
| 2 | 0.75 | 1.0 | 0.985 | 0.986 |
| 5 | 0.75 | 1.0 | 0.928 | 0.931 |
| 1 | 0.75 | 2.0 | 0.946 | 0.944 |
| 2 | 0.75 | 2.0 | 0.940 | 0.938 |
| 5 | 0.75 | 2.0 | 0.903 | 0.900 |
| 1 | 0.5 | 0.25 | 1.139 | 1.128 |
| 2 | 0.5 | 0.25 | 1.098 | 1.089 |
| 5 | 0.5 | 0.25 | 0.931 | 0.927 |
| 1 | 0.5 | 1.0 | 0.991 | 0.992 |
| 2 | 0.5 | 1.0 | 0.970 | 0.971 |
| 5 | 0.5 | 1.0 | 0.868 | 0.868 |
| 1 | 0.5 | 2.0 | 0.897 | 0.892 |
| 2 | 0.5 | 2.0 | 0.886 | 0.879 |
| 5 | 0.5 | 2.0 | 0.815 | 0.811 |

† To minimise the effects of a possible error of the order of one per cent. in Crocco's calculations, ratios rather than absolute values of skin friction coefficients are compared.

$$\text{heat transfer} = T_1\left[1+\frac{(\gamma-1)}{2}M_1^2\sigma^{\frac{1}{2}}\right].$$

If we now use equation (36) to derive $S_F$ and $\tau_w$, we find

$$S_F = 0.664\frac{\rho_1 u_1^2 L}{\sqrt{(u_1 L/\nu)}}[0.45+0.55\,i\,(0)+0.09\,(\gamma-1)\,M_1^2\sigma^{\frac{1}{2}}]^{-\frac{1-\omega}{2}} \quad . \quad (39)$$

and

$$\tau_w = 0.332\frac{\rho_1 u_1^2}{\sqrt{(u_1 x/\nu_1)}}[0.45+0.55\,i\,(0)+0.09\,(\gamma-1)\,M_1^2\sigma^{\frac{1}{2}}]^{-\frac{1-\omega}{2}}. \quad . \quad (40)$$

Equations (38), (39) and (40) enable us to calculate $q$ and $Q$ in any case where $T_w, T_1, M_1, \sigma$ and $\omega$ are given.

### 3.2. *Effect of radiation on thermometer temperature*

The following treatment is a modification of that due to Hantzsche and Wendt[3], use being made of the explicit formula for $F(0)$, equation (36).

Allowing for the radiation of heat in the thermometer problem, then the rate of

TABLE II

Comparison of Crocco's calculated values of skin friction on a flat plate with values given by equation (37) for case of zero heat transfer ($\sigma = 0.725$).

| $M_1$ | $\omega$ | $\frac{c_f\sqrt{R_x}}{(c_f\sqrt{R_x})_{\omega=1}}$ | $\frac{c_f\sqrt{R_x}}{0.664}$ (Equation (37)) |
|---|---|---|---|
| 1 | 1.25 | 1.015 | 1.015 |
| 2 | 1.25 | 1.053 | 1.052 |
| 5 | 1.25 | 1.194 | 1.193 |
| 1 | 0.75 | 0.984 | 0.986 |
| 2 | 0.75 | 0.950 | 0.951 |
| 5 | 0.75 | 0.842 | 0.838 |
| 1 | 0.5 | 0.969 | 0.971 |
| 2 | 0.5 | 0.908 | 0.904 |
| 5 | 0.5 | 0.707 | 0.702 |

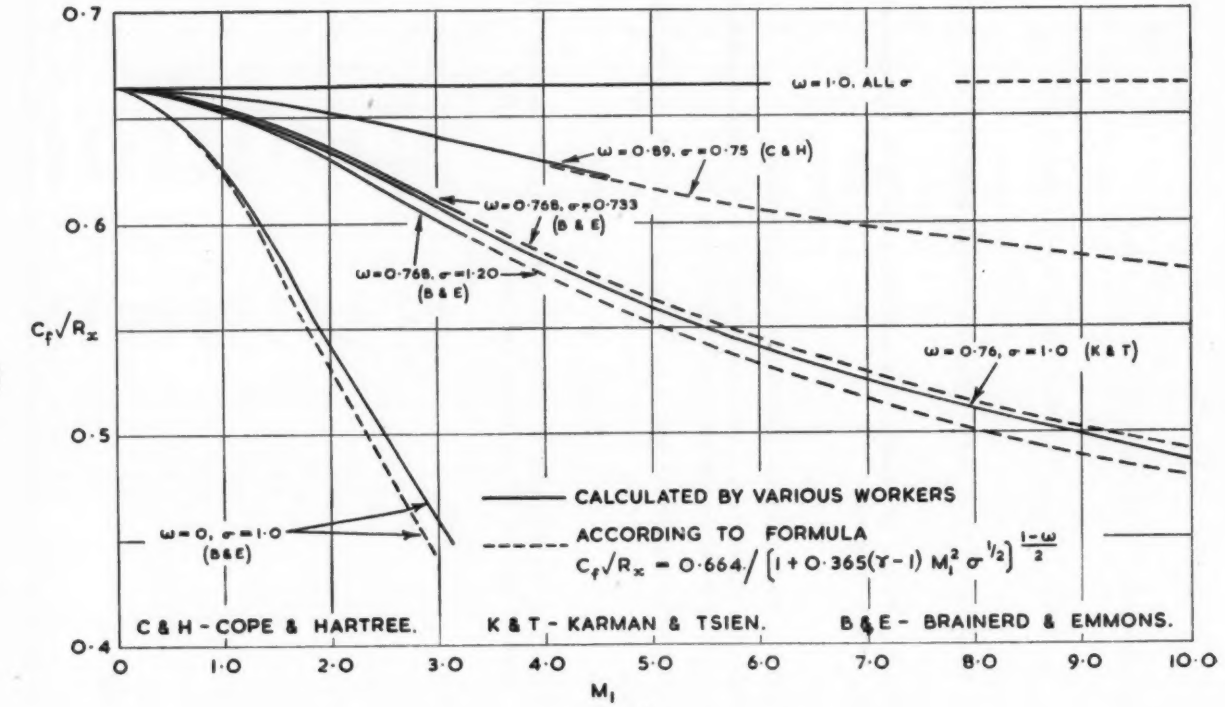


Fig. 2.
Skin friction on a flat plate at zero incidence. No heat transfer.

heat transfer from gas to wall must equal the rate at which heat is radiated. Hence

$$Q=\int_0^L C_B(T_1^4-T_w^4)\,dx,$$

where $C_B$=Stefan-Boltzmann's constant multiplied by the emissivity.

Using equation (38) we have therefore

$$\frac{c_p(T_w-T_{th})}{\sigma^{2/3}u_1}\frac{2F(0)}{\sqrt{R_L}}\tfrac{1}{2}\rho_1u_1^2L=C_BL(T_w^4-T_1^4),$$

or

$$\frac{\left[i(0)-1-\dfrac{(\gamma-1)}{2}M_1^2\sigma^{\frac{1}{3}}\right]}{\sigma^{2/3}(i(0)^4-1)}F(0)\,c_p(u_1\rho_1\mu_1/L)^{\frac{1}{2}}=C_BT_1^3.$$

Write

$$K_R=\frac{C_BT_1^3L}{c_pR_L^{\frac{1}{2}}\mu_1}. \qquad (41)$$

Then

$$K_R=\frac{\left[i(0)-1-\dfrac{(\gamma-1)}{2}M_1^2\sigma^{\frac{1}{3}}\right]}{\sigma^{2/3}[i(0)^4-1]}F(0),$$

where, as before, we have

$$F(0)=0.664\,[0.45+0.55\,i(0)+0.09M_1^2\sigma^{\frac{1}{3}}]^{-\frac{(1-\omega)}{2}} \qquad (42)$$

The problem is, in general, given $K_R$, what is the value of $i(0)$? With the aid of equation (46) the problem is best treated in reverse; that is, for given values of $M_1$, $\omega$, $\sigma$ and $i(0)$ the corresponding values of $K_R$ can be calculated and the values of $i(0)$ can be plotted against $K_R$. We may note immediately that for $K_R=0$ (as when $L=0$), $T_w=T_{th}$, for $K_R=\infty$ (as when $L=\infty$), $i(0)=1$, *i.e.* $T_w=T_1$. For intermediate values, $i(0)$ decreases steadily with increase of $K_R$.

## 4. THE LAMINAR BOUNDARY LAYER ON A CYLINDER

The method to be developed here is essentially the same as a method previously put forward by the author[11], but with a number of improvements suggested by the results given in Section 2.

Suffix 0 will be used to denote undisturbed stream values, and suffix 1 to denote values just outside the boundary layer.

The momentum equation of the boundary layer is readily shown to be[11]

$$\theta'+\left[(H+2)\frac{u_1'}{u_1}+\frac{\rho_1'}{\rho_1}\right]\theta=\frac{\tau_w}{\rho_1u_1^2}, \qquad (43)$$

where $$\theta = \int_0^\infty \frac{\rho u}{\rho_1 u_1}\left(1 - \frac{u}{u_1}\right) dy, \quad \delta^{**} = \int_0^\infty \left(1 - \frac{\rho u}{\rho_1 u_1}\right) dy,$$

$H = \delta^{**}/\theta$, and dashes denote differentiation with respect to $x$, the distance along the surface.

We will now follow some of the implications of an approach on the lines of Pohlhausen's method for incompressible flow. Instead of expressing the velocity distribution as a function of $y$, however, it will be expressed as a function of $Y = \int \frac{\mu_0 dy}{\mu}$, since we know that on a flat plate, with $\omega = 1.0$, the velocity distribution expressed as a function of $Y$ is independent of Mach number. Thus, suppose the velocity distribution across the boundary layer to be given by the quartic

$$u = aY + bY^2 + cY^3 + dY^4, \quad . \quad . \quad . \quad . \quad . \quad (44)$$

with the boundary conditions that

$$\text{for } Y = \delta_1^*, \; u = u_1, \; \frac{\partial u}{\partial Y} = \frac{\partial^2 u}{\partial Y^2} = 0;$$

$$\text{and for } Y = 0, \; u = 0, \; \frac{\partial T}{\partial Y} = 0, \text{ and hence } \frac{\partial \mu}{\partial Y} = 0.$$

The quantity $\delta_1^*$ is at present unknown, but is assumed to correspond to the value of $Y$ defining the outer edge of the boundary layer.

The first boundary layer equation yields

$$\frac{\partial}{\partial y}\left(\mu \frac{\partial u}{\partial y}\right)_w = \frac{\partial p}{\partial x} = -\rho_1 u_1 u_1'.$$

But $$\frac{\partial}{\partial y}\left(\mu \frac{\partial u}{\partial y}\right)_w = \mu_w \left(\frac{\partial^2 u}{\partial y^2}\right)_w, \text{ since } \left(\frac{\partial \mu}{\partial y}\right)_w = 0,$$

$$= \frac{\mu_0^2}{\mu_w}\left(\frac{\partial^2 u}{\partial Y^2}\right)_w.$$

Hence $$\left(\frac{\partial^2 u}{\partial Y^2}\right)_w = -\frac{\mu_w}{\mu_1^2} \cdot \rho_1 u_1 u_1'.$$

With these boundary conditions we can solve for the coefficients $a$, $b$, $c$ and $d$ in terms of $\delta_1^*$, and we obtain

$$\left.\begin{aligned} a=\frac{u_1(12+\Lambda)}{6\delta_1^*},\ b=\frac{-u_1\Lambda}{2\delta_1^{*2}},\ c=\frac{-u_1(4-\Lambda)}{2\delta_1^{*3}},\ d=\frac{u_1(6-\Lambda)}{6\delta_1^{*4}}, \\ \text{where}\qquad \Lambda=u_1'\delta_1^{*2}\rho_1\frac{\mu_w}{\mu_0^2}. \end{aligned}\right\} \quad . \quad (45)$$

Further, since $$\tau_w=\mu_w\left(\frac{\partial u}{\partial y}\right)_w=\mu_0\left(\frac{\partial u}{\partial Y}\right)_w,$$

$$\frac{\tau_w}{\rho_1 u_1^2}=\frac{\mu_0(12+\Lambda)}{6\rho_1 u_1\delta_1} \quad . \quad . \quad . \quad . \quad . \quad . \quad . \quad (46)$$

From this point the method departs from the classical Pohlhausen approach. It depends on the solution of the momentum equation, making the following assumptions

(*i*) Equation (46) is accepted.

(*ii*) The variation of $H$ with local velocity, pressure gradient, $\omega$ and $\sigma$ is neglected, $H$ being treated as a function of $M_0$ only. The justification for this lies in the fact that $H$ enters the solution of the momentum equation in a form suggesting that the solution is relatively insensitive to small variations of $H$, and for slim bodies at small incidences the possible variations of $H$ are unlikely to be large.†

For a flat plate at zero incidence, with $\omega$ and $\sigma$ both unity we know that $u/u_0$ is a unique function of $Y$, and also the total energy is constant across the boundary layer. Hence, in this case

$$\theta=\int_0^\infty\frac{\rho u}{\rho_0 u_0}\left(1-\frac{u}{u_0}\right)dy=\int_0^\infty\frac{u}{u_0}\left(1-\frac{u}{u_0}\right)dY=\theta_i,$$

where suffix "i" denotes the value in incompressible flow.

Also $$\delta^{**}=\int_0^\infty\left(1-\frac{\rho u}{\rho_0 u_0}\right)dy=\int_0^\infty\left(\frac{\mu}{\mu_0}-\frac{u}{u_0}\right)dY.$$

But $$\frac{\mu}{\mu_0}=\frac{T}{T_0}=1+\frac{(\gamma-1)}{2}M_0^2\left(1-\frac{u^2}{u_0^2}\right).$$

† It is possible to avoid making this assumption, but the computing involved then becomes considerably heavier.

Hence $$\delta^{**}=\int_0^\infty \left(1-\frac{u}{u_o}\right)dY+\frac{(\gamma-1)M_o^2}{2}\int_0^\infty\left(1-\frac{u^2}{u_o^2}\right)dy$$

$$=\delta_1^{**}+\frac{(\gamma-1)}{2}M_o^2(\delta_1^{**}+\theta_1).$$

Therefore

$$H=\frac{\delta^{**}}{\theta}=H_1\left\{1+\frac{(\gamma-1)}{2}M_o^2\left(1+\frac{1}{H_1}\right)\right\}.$$

The Blasius solution gives

$$H_1=2.59,$$

hence $$H=2.59\,(1+0.277M_o^2). \quad . \quad . \quad . \quad . \quad . \quad . \quad . \quad (47)$$

This relation is in almost exact agreement with the results of the calculations of Brainerd and Emmons[4].

(*iii*) The ratio $\delta_1^*/\theta$ is also assumed to be independent of variations in local velocity and pressure gradient. For the present we write

$$\delta_1^*/\theta=\mathrm{f}\,(M_o,\ \omega,\ \sigma)\dagger \quad . \quad . \quad . \quad . \quad . \quad (48)$$

making no further assumptions at this stage about the form of the function, except to note that we expect it to be constant when $\omega=1.0$.

From (46) and the expression for $\Lambda$ in (45) we have

$$\frac{\tau_w}{\rho_1 u_1^2}=\frac{\mu_o}{6\rho_1 u_1\delta_1^*}\left[u_1'\delta_1^{*2}\rho_1\frac{\mu_w}{\mu_o^2}+12\right]$$

$$=\frac{u_1'}{6u_1}\delta_1^*\frac{\mu_w}{\mu_o}+\frac{2\mu_o}{\rho_1 u_1\delta_1^*}$$

$$=\frac{u_1'}{6u_1}\frac{\mu_w}{\mu_o}f\theta+\frac{2\mu_o}{\rho_1 u_1 f\theta}.$$

Hence, the momentum equation (42) becomes

$$\theta'+\left[(H+2)\frac{u_1'}{u_1}+\frac{\rho_1'}{\rho_1}\right]\theta=\frac{u_1'}{6u_1}\frac{\mu_w}{\mu_o}f\theta+\frac{2\mu_o}{\rho_1 u_1 f\theta}.$$

† This function should not be confused with the function $f$ of equation (6).

Multiply both sides by $\rho_1{}^2\theta$, and we get

$$\frac{d}{dx}[\rho_1{}^2\theta^2]+2\rho_1{}^2\theta^2\frac{u_1'}{u_1}\left[(H+2)-\frac{\mathrm{f}}{6}\frac{\mu_w}{\mu_o}\right]=4\frac{\mu_o\rho_1}{u_1\mathrm{f}} \quad . \quad . \quad . \quad (49)$$

At this stage a further assumption is made, *viz.* the value of $\mu_w/\mu_o$ in the second bracket is taken to be that for a flat plate at zero incidence. This gives

$$\frac{\mu_w}{\mu_o}=\left[1+\frac{(\gamma-1)}{2}\sigma^3M_o^2\right]^\omega \quad . \quad . \quad . \quad . \quad (50)$$

Write $$H+2-\frac{\mathrm{f}}{6}\cdot\frac{\mu_w}{\mu_o}=\mathrm{g}\,(M_o,\,\omega,\,\sigma)/2, \text{ say.} \quad . \quad . \quad . \quad (51)$$

Then (49) can be integrated with respect to $x$ to yield

$$\left[u_1{}^{\mathrm{g}}\rho_1{}^2\theta^2\right]_0^{x_1}=\frac{4}{\mathrm{f}}\mu_o\int_0^{x_1}\rho_1u_1{}^{\mathrm{g}-1}dx \quad . \quad . \quad . \quad . \quad (52)$$

The leading edge is taken at $x=0$, where either $u_1=0$, or $u_1$ is finite. If $u_1$ is finite, then $\theta=0$ there, since we cannot have a finite momentum loss there. Hence

$$[\rho_1{}^2\theta^2]_{x_1}=\frac{4\mu_o}{\mathrm{f}u_1\,(x_1)^{\mathrm{g}}}\int_0^{x_1}\rho_1u_1{}^{\mathrm{g}-1}dx. \quad . \quad . \quad . \quad (53)$$

We may note here that g occurs as an exponent of $u_1$ inside the integral, and as an exponent of $u_1\,(x_1)$ outside the integral in the denominator. This suggests that provided the variation of $u_1$ with $x$ is small, small errors in g will have little effect, and this provides the justification for the neglect of the variation of $H$ and $\mu_w/\mu_o$ with pressure gradient and local velocity.

We have yet to determine the function f.

For the flat plate at zero incidence (53) reduces to

$$[\rho_o\theta^2]_{x_1}=\frac{4\mu_ox_1}{u_o\mathrm{f}}$$

or $$\frac{\theta\sqrt{R_x}}{2x}=\sqrt{\left(\frac{1}{\mathrm{f}}\right)},$$

and $$\frac{\partial\theta}{\partial x}=\frac{1}{\sqrt{R_x}}\frac{1}{\sqrt{\mathrm{f}}}.$$

But $$c_f = \frac{2\tau_w}{\rho_o u_o^2} = 2\frac{\partial \theta}{\partial x}$$

$$= \frac{2}{\sqrt{R_x}} \cdot \frac{1}{\sqrt{f}}.$$

Hence $\frac{2}{\sqrt{f}} = c_f\sqrt{R_x} = 0.664\,[1+0.365\,(\gamma-1)\,\sigma^{\frac{1}{3}}M_o^2]^{\frac{\omega-1}{2}}$, from equation (37).

It follows that

$$f = 9.072\,[1+0.365\,(\gamma-1)\,\sigma^{\frac{1}{3}}M_o^2]^{1-\omega}. \quad . \quad . \quad . \quad (54)$$

The function g is given by

$$g = 2\,(H+2) - \frac{f}{3}\frac{\mu_w}{\mu_o}$$

$$= 9.18 + 1.436M_o^2 - \frac{f}{3}\left[1+\frac{(\gamma-1)}{2}\sigma^{\frac{1}{3}}M_o^2\right]^{\omega}. \quad . \quad . \quad (55)$$

It is sometimes convenient to express these relations in non-dimensional forms.

Thus, write $$\rho^* = \frac{\rho}{\rho_o},\ \mu^* = \frac{\mu}{\mu_o},\ u^* = \frac{u}{u_o},\ \theta^* = \frac{\theta}{L},\ x^* = \frac{x}{L},$$

where $L$ is some standard length, then (53) becomes

$$[\rho_1^{*2}\theta^{*2}]_{x_1} R = \frac{4}{u_1(x_1^*)^{\xi} f}\int_0^{x_1} \rho_1^* u_1^{*(\xi-1)} dx^*, \quad . \quad . \quad . \quad (56)$$

where $R = \mu_o L/\nu_o$.

The relation between $\rho_1^*$ and $u_1^*$ is

$$\rho_1^* = \left[1+\frac{(\gamma-1)}{2}M_o^2\,(1-u_1^{*2})\right]^{\frac{1}{\gamma-1}}. \quad . \quad . \quad . \quad (57)$$

Having $u_1^*$ as a function of $x^*$, we can then obtain $\theta^*$ at any point from equations (54), (55), (56) and (57), the solution of (56) being obtained by graphical or numerical integration.

To obtain the local skin friction coefficient when $\theta^*$ is known, we have

$$\left.\begin{aligned} c_f &= \frac{2\tau_w}{\rho_o u_o^2} = \frac{(\Lambda+12)\,u_1}{3R\theta^* \mathrm{f}} \\ \text{and} \quad \Lambda &= u_1'\delta_1^{*2}\rho_1 \frac{\mu_w}{\mu_o^2} \\ &= R\,(u_1^{*\prime}\theta^{*2}\mathrm{f}^2\rho_1^*\mu_w^*). \end{aligned}\right\} \quad . \quad . \quad . \quad . \quad . \quad (58)$$

For $\mu_w^* = \mu_w/\mu_o$, we may use equation (50) but it is probably more accurate at this point to assume that the local relation between $T_w$, $T_1$ and $u_1$, is the same as for the flat plate which leads to the relation[16]

$$\mu_w^* = \left\{1 + \frac{(\gamma-1)}{2} M_o^2 \left[1 + \frac{u_1^2}{u_o^2}(\sigma^{\frac{1}{2}} - 1)\right]\right\}^{\omega}. \quad . \quad . \quad . \quad . \quad (59)$$

The accuracy of the method outlined above cannot as yet be assessed; this must await the development of a method that can be accepted as accurate and its application to a few test cases. In favour of the above method it should be noted that it gives the correct answer for the flat plate at zero incidence and the numerical work involved in its application is relatively small. It may also be noted that when applied to incompressible flow[11] the method gave results which were in very close agreement with results given by the standard Pohlhausen method.

## 5. SEPARATION OF THE BOUNDARY LAYER

It is unlikely that the above method will be any more successful in predicting the separation point of the laminar boundary layer than is the Pohlhausen method in incompressible flow. Nevertheless, it should provide a guide as to the effect of increase of Mach number on tendency to separation.

From (45) separation occurs when $\Lambda = -12$, *i.e.* when

$$R\theta^{*2}\rho_1 = \frac{-12}{u_1^{*\prime}\mathrm{f}^2\mu_w^*}, \text{ from (58).}$$

Hence, from (56), separation occurs at $x_1$, if

$$\left[\frac{-3u_1^{*z}\rho_1^*}{u_1^{*\prime}\mathrm{f}\mu_w^*}\right]_{x_1} = \int_0^{x_1^*} \rho_1^* u_1^{*z-1} dx^*. \quad . \quad . \quad . \quad . \quad (60)$$

Howarth has considered the case of a uniform adverse velocity gradient with $\omega = 1.0$ and $\sigma = 1.0$, and has estimated the separation distance for different main stream Mach numbers at the beginning of the plate, using a method that is essentially an

analogue of Pohlhausen's method. It is of interest to compare his results with the results given by the present method.

With $\omega = 1.0$, and $\sigma = 1.0$,

$$f = 9.072, \quad g = 6.156 + 0.831 M_o^2, \text{ and } \mu_w^* = 1 + \tfrac{1}{2}(\gamma - 1) M_o^2.$$

Suppose $u_1 = u_o - \beta x$, where $\beta$ is a constant.

Then $u_1^* = 1 - \dfrac{\beta L}{u_o} x^*$, and $u_1^{*\prime} = -\dfrac{\beta L}{u_o} = \alpha$, say.

Equation (60) becomes

$$\frac{3}{9.072\left(1 + \dfrac{(\gamma-1)}{2} M_o^2\right)\alpha} = \frac{1}{(1 - \alpha x_1^*)^g \rho_1^*(x_1)} \int_0^{x_1^*} \rho_1^* (1 - \alpha x^*)^{g-1} dx^*$$

and, from (57)

$$\rho_1^* = \left[1 + \frac{(\gamma-1)}{2} M_o^2 (2\alpha x^* - \alpha^2 x^{*2})\right]^{\frac{1}{\gamma-1}}.$$

Let $\alpha x^* = s$, then we have

$$0.331 = \frac{\left[1 + \dfrac{(\gamma-1)}{2} M_o^2\right]}{(1 - s_1)^g \left[1 + \dfrac{(\gamma-1)}{2} M_o^2 (2s_1 - s_1^2)\right]^{\frac{1}{\gamma-1}}} \times$$

$$\times \int_0^{s_1} \left[1 + \frac{(\gamma-1)}{2} M_o^2 (2s - s^2)\right]^{\frac{1}{\gamma-1}} (1 - s)^{g-1} \, ds, \quad . \quad . \quad (61)$$

with $g = 6.156 + 0.831 M_o^2$.

The process is then, given $M_o$, to evaluate the right hand side numerically for a range of values of $s_1$, and to interpolate to obtain the value of $s_1$ for which (61) is satisfied.

The results for the separation distance $x_s$ given by this method are compared with those given by Howarth's method in the following table:—

| | $-\beta x_s/u_0$ | |
|---|---|---|
| $M_0$ | *Howarth* | *Present method* |
| 0 | 0.156 | 0.165 |
| 1 | 0.148 | 0.148 |
| 3.16 | 0.107 | 0.081 |
| 10 | 0.052 | 0.013 |

The agreement between the two methods is poor for the higher Mach numbers, but neither method can be claimed *a priori* as very reliable for predicting the point of separation, and it is impossible at this stage to estimate their relative degrees of reliability for this purpose†. It can be inferred from both sets of results, however, that the separation point moves forward with increase of initial Mach number for constant $\frac{\beta}{u_0} = -\frac{du}{dx} \Big/ u_0$, *i.e.* for constant ratio of (velocity fall per unit length of plate) to (initial velocity).

## REFERENCES

1. BUSEMANN, A. (1935). Gasströmung mit laminarer Grenzschicht entlang einer Platte. *Z.A.M.M.*, Vol. 15, Feb. 1935.

2. KÁRMÁN, TH. VON, and TSIEN, H. S. (1937). Boundary Layers in Compressible Fluids. *Journal Aero. Sciences*, Vol. 15, 1937-38.

3. HANTZSCHE, W., and WENDT, H. (1940). Zum Kompressibilitätseinfluss bei der laminaren Grenzschicht der ebenen Platte. *Jahrbuch der Deutschen Luftfahrtforschung*, 1940, I., p. 517.
Die laminare Grenzschicht der ebenen Platte mit und ohne Wärmeübergang. *Jahrbuch der Deutschen Luftfahrtforschung*, 1941, I., p. 40.

† *Note added in proof.* The author's attention has been drawn to a paper by Stewartson, as yet unpublished, in which a complete transformation is established between a boundary layer in compressible flow, $\omega = 1.0$, $\sigma = 1.0$, with a given external velocity distribution and an incompressible flow boundary layer with a related external velocity distribution. Consequently, all accepted solutions for the incompressible flow boundary layer can be transformed to yield solutions of equal accuracy in compressible flow with $\omega$ and $\sigma$ both equal to unity. The problem considered above is readily solved using the corresponding "series" solution in incompressible flow, and the values of the non-dimensional distance to separation calculated by Stewartson for the four values of $M_0$ quoted above are 0.120, 0.114, 0.075 and 0.024.

4. EMMONS, H. W., and BRAINERD, J. G. (1941). Temperature Effects in a Laminar Compressible Fluid Boundary Layer along a Flat Plate. *J. App. Mechanics*, Sept. 1941, Vol. 8, No. 3, A.R.C. 5400.
Effect of Variable Viscosity on Boundary Layers, with a Discussion of Drag Measurements. A.S.M.E. Preprint, June 1941, A.R.C. 5498.

5. COPE, W. F., and HARTREE, D. R. (1948). The Laminar Boundary Layer in Compressible Flow. *Phil. Tran. Roy. Soc.*, A., Vol. 241, pp. 1-69, June 1948.

6. CROCCO, L. (1946). Lo Strato Limité Laminare nei Gas. Monografic Scientifiche di Aeronautica, No. 3, Dec. 1946, A.R.C. 11,453.

7. HOWARTH, L. (1938). *Proc. Roy. Soc.*, A.164, 1938, pp. 547-579.

8. HOWARTH, L. (1947). Concerning the Effect of Compressibility on Laminar Boundary Layers and their Separation. A.R.C. 10,821, 1947, to appear in *Proc. Roy. Soc.*

9. FRANKL, F. (1934). Theory of Laminar Boundary Layers in Compressible Gases. R.T.P. Trans., 469, A.R.C. 3113, 1934.

10. OSWATITSCH, K. L., and WIEGHARDT, K. (1946). Theoretical Investigations on Steady Potential Flows and Boundary Layers at High Speeds. R. & T., No. 187, A.R.C. 10,378. 1946.

11. YOUNG, A. D., and WINTERBOTTOM, N. E. (1940). Note on the Effect of Compressibility on the Profile Drag of Aerofoils in the Absence of Shock Waves. A.R.C. 4697, 1940.

12. ILLINGWORTH, C. R. (1946). The Laminar Boundary Layer Associated with the Retarded Flow of a Compressible Fluid. A.R.C. 9886, 1946.

13. Edited by GOLDSTEIN, S. (1938). *Modern Developments in Fluid Dynamics*. Vol. I., p. 156—.

14. COPE, W. F. (1945). Note on the Law of Variation of Viscosity and on the Prandtl Number of Air at Low Temperatures. A.R.C. 9287, 1945.

15. Edited by GOLDSTEIN, S. (1938). *Modern Developments in Fluid Dynamics*. Vol. II., p. 627—.

16. SQUIRE, H. B. (1942). Heat Transfer Calculation for Aerofoils. R. & M. 1986, 1942.

# THE MEASUREMENT OF GAS TURBINE COMBUSTION EFFICIENCY BY GAS ANALYSIS

by

L. J. RICHARDS AND J. C. STREET

*(Thornton Research Centre, Shell Refining and Marketing Company Limited)*

SUMMARY

Following a brief discussion of various methods of measuring combustion efficiency in gas turbine chambers, the superiority in accuracy of applied gas analysis is stated. Factors leading to inefficiencies in combustion are outlined and the exhaust constituents requiring measurement are deduced. The chief difficulty in the past in the application of gas analysis methods to combustion efficiency determination has been the time consumed in actual analysis of samples; at Thornton Research Centre means of overcoming this difficulty have been investigated and several rapid and accurate analytical techniques have been developed and used successfully. These techniques are described, together with other promising methods at present under development. The broad requirements of obtaining exhaust gas samples for analysis are discussed and typical sampling systems described; precautions necessary in applying these systems are given. Formulæ for the calculation of combustion efficiency from analytical results, together with any assumptions made, are given in the text and their derivation explained in an Appendix. The techniques described have been developed primarily for use in conjunction with rig testing of aircraft gas turbine combustion chambers; the broader application—for instance, to engine testing—of the principles involved are considered briefly.

## 1. INTRODUCTION

It is well known that in the development and testing of gas turbine combustion chambers, one of the most important performance criteria requiring evaluation is "combustion efficiency"—a measure of the proportion of the total fuel supplied usefully employed in giving energy to the working gases of the turbine.

The variety of methods by which measurement of combustion efficiency has

Paper received January 1949.

[The Aeronautical Quarterly, Vol. 1, August 1949]

been attempted has resulted in several different conceptions and definitions of this term, but since the primary considerations are those of heat or energy, perhaps the one most appropriate, and therefore adopted in this paper, is the ratio of the heat actually developed in the chamber to the heat which would be developed by complete combustion of all the fuel supplied to the chamber. In the experimental determination of combustion efficiency, calculation of the maximum heat or energy available is based on the calorific value and rate of supply of fuel to the combustion chamber on test, but measurement of the actual heat generated has been attempted in several ways, the most important of which are:—

(*i*) by combustion chamber thrust measurement

(*ii*) by measuring gas temperature rise in the combustion chamber

(*iii*) by chemical analysis of the combustion chamber exhaust gases and computation of efficiency from the measured quantities of various constituents.

In the combustion chamber thrust measurement, efficiency is determined by comparing the actual thrust, obtained under given chamber operating conditions, with the theoretical maximum thrust calculated from fuel and air supply rates, calorific value of the fuel, and the exhaust nozzle dimensions. Direct comparison on these lines will not give values of combustion efficiency in accordance with the earlier definition, but will include the aerodynamic efficiency of the chamber. Further tests to determine the pressure loss characteristics of the combustion system will enable combustion efficiency to be partially separated from the combined term, but the validity of utilising "cold" pressure loss data in the correction of experimental results obtained with high temperature gases is doubtful. The method then, although perhaps of use for tests of comparison, cannot yield results of any great absolute accuracy. Probably the most important disadvantages in the application of the principle are the mechanical difficulties involved; obviously, for any acceptable degree of accuracy small changes in thrust must be readily detectable, and the physical proportions of the necessary flexible air ducts, etc., leading to the chamber militate against this. It can be said, then, that thrust measurement shows little promise as an accurate means of combustion efficiency measurement, and is at present rarely used for that purpose.

By far the most widely used method for the evaluation of combustion efficiency is that of measuring the gas temperature rise in the combustion chamber and comparing the results with the theoretical value based on complete combustion. A direct comparison of such temperature increments results in a value of efficiency slightly different from that given by the "energy" definition, because of variations with temperature in the specific heats of the gases under study, but in most practical cases numerical discrepancies are negligible, particularly at high values of efficiency. The practical application of this principle requires the measurement of gas temperature at the outlet of the combustion chamber where, unfortunately, the

temperature and gas velocity distributions are seldom uniform. Common practice, then, is to traverse the outlet of the combustion chamber with a suitable thermocouple and pitot-static instrument and thus obtain a mean value of the outlet gas temperature weighted according to gas velocity distribution. The necessity of such a procedure is the prime factor in limiting the accuracy of this method; the accurate measurement of high gas temperatures in rapidly moving streams is a problem in itself, while, because of the steep temperature gradients frequently occurring across the chamber outlet the estimated mean value of indicated gas temperature is often open to doubt. Further errors must be expected in estimating the maximum gas temperature rise available from the fuel supplied, for this must be calculated from measured air and fuel supply rates, both of which are limited in accuracy, particularly the former.

So far only the unfavourable characteristics of the " heat balance " technique have been discussed, but its wide application testifies to its general value. In the hands of experienced personnel, the method can be made relatively speedy and reliable within known limits of accuracy and, although perhaps not suited for highly accurate determination of, or the detection of small changes in, combustion efficiency, it is at present the most convenient tool for general combustion chamber development.

Where a high degree of accuracy is required in efficiency determination, exhaust gas analysis methods are unsurpassed, being both sensitive and accurate on an absolute standard. The principles involved consist broadly in the estimation of both the heat actually released and the maximum heat available in the combustion chamber from the composition of the exhaust gases, and in some circumstances no other measurements are necessary. One of the chief objections in the application of these principles, however, has been the time consumed in the analysis of samples, and much effort has been expended in recent years in devising rapid analytical techniques of the required precision. In this paper some of the more successful results of such work at Thornton Research Centre are summarised, and their application in the determination of combustion efficiency in aircraft gas turbine combustion chambers is described; analytical methods envisaged for future use or at present under development are also included.

## 2. THE PROBLEM

In contemporary combustion chambers, because of practical limitations, the combustion process is never theoretically complete. This means that a proportion of the total available heat is not released; this unavailable heat is known as the combustion loss.

Several factors contribute to the combustion loss, the more important of which are:—

(*i*) The chilling of the combustion reactions occurring in the primary zone, mainly by the admission of the secondary and tertiary air.

(*ii*) Slow or delayed combustion, which is usually caused by bad mixing in the primary zone and is often indicated by a long flame. This will cause the effect of the chilling to be much more severe, as the reaction will be chilled at an earlier stage.

The above two factors will cause the presence in the exhaust gas of partially burnt products.

(*iii*) Failure to ignite some of the fuel or products of the secondary reactions, *i.e.* cracking products. This again may be due to imperfect mixing conditions in the primary zone. This factor will result in unburnt fuel, as well as partially burnt products, appearing in the exhaust gas.

Taking into account these various mechanisms, the likely constituents of the exhaust which contribute to combustion loss are:—

(*a*) Hydrocarbons (unburnt fuel, cracked fuel, and so on)

(*b*) Carbon monoxide

(*c*) Hydrogen

(*d*) Other intermediate combustion products (aldehydes, acids, peroxides)

(*e*) Carbon.

The relative importance of these may vary considerably with the combustion chamber operating conditions, but generally speaking the first three are by far the most important. The amount of carbon formed even under heavy coking conditions corresponds to a thermal loss of 0.1 per cent.[1] or less of the total available heat and may be neglected. Peroxides have not been detected in normal combustion. Formaldehyde and formic acid[2] can be detected by direct chemical methods, but again their contribution is normally not significant ($< 0.1$ per cent.). Even when the total loss is large and their contribution rises to about 0.3 per cent., this still forms a very small fraction of the total loss and may be neglected. For purposes of rapidity and simplicity, therefore, constituents (*d*) and (*e*) may be neglected for all practical determinations of combustion efficiency.

In all determinations of combustion efficiency on gas turbine combustion chambers, there is a conflict between two factors, *i.e.* rapidity and accuracy. A complete and comprehensive analysis could be made of every possible exhaust gas constituent, which would enable the combustion efficiency to be determined with very high accuracy, but the time involved would be far too long and this would not be practicable as a routine test. Also, the accuracy obtained would probably be meaningless because the overall accuracy is controlled by the difficulty of obtaining a truly representative sample of the exhaust gases.

Accordingly, bearing in mind the necessity of maintaining an accuracy commensurate with the requirements of the test, various approximations may be made which will enable the determination of efficiency to be made with greater rapidity than

otherwise. Thus, as stated above, the loss due to carbon, aldehydes, acids and peroxides may be neglected. This means that the exhaust gas must be accurately analysed for hydrogen, carbon monoxide and hydrocarbons. The method of calculation of combustion efficiency from the analytical results, as well as the various approximations which may be used, are shown in Appendix I and discussed in a later Section. If the requirements of the test permit, an approximation to efficiency may be made by neglecting the hydrogen, which normally is only present in small amounts, and by measuring the loss caused by carbon monoxide and hydrocarbons alone.

Finally, if rapidity is of the utmost importance, as is often the case in routine work, instead of determining the actual thermal efficiency an estimate of this efficiency may be made by determining the $CO_2$ combustion efficiency. This may be defined as:—

$$\frac{\text{Percentage by volume of } CO_2 \text{ in exhaust gas}}{\text{Theoretical percentage by volume of } CO_2 \text{ for complete combustion to } CO_2 \text{ and } H_2O}$$

This "efficiency" will normally be lower than the true efficiency because it involves treating the intermediate combustion products as a total loss, whereas in fact they are not so; for instance, the formation of carbon monoxide is accompanied by some heat release. The fact that the presence of any free hydrogen in the exhaust gases has been neglected would tend to minimise this discrepancy. The relative efficiencies obtained when comparing various fuels and conditions are not greatly affected by the above approximations, and the rapidity with which results may be obtained is greatly increased since, in the case of the $CO_2$ combustion efficiency, as will be shown later, all that is required is two determinations on the exhaust gas for carbon dioxide.

## 3. ANALYTICAL METHODS FOR MEASURING IMPORTANT CONSTITUENTS OF LOSS

This Section represents a brief survey of some possible methods for the determination of constituents of the exhaust gas which are important in combustion efficiency determination. For consideration of space the methods are not described in detail, emphasis being placed mainly on the principles involved.

### *3.1. Cambridge vacuum method*[3]

This method is primarily used for the estimation of gases which contain carbon in the molecule, although the analysis does include an estimation of oxygen and nitrogen. The layout of the apparatus is shown diagrammatically in Fig. 1. The principle of the method is simply, by fractional combustion, to convert in turn each carbon-containing constituent or group of constituents to carbon dioxide ($CO_2$), to condense the $CO_2$ so formed and, after distillation, to measure the amount of this $CO_2$ by the pressure exerted in a known volume.

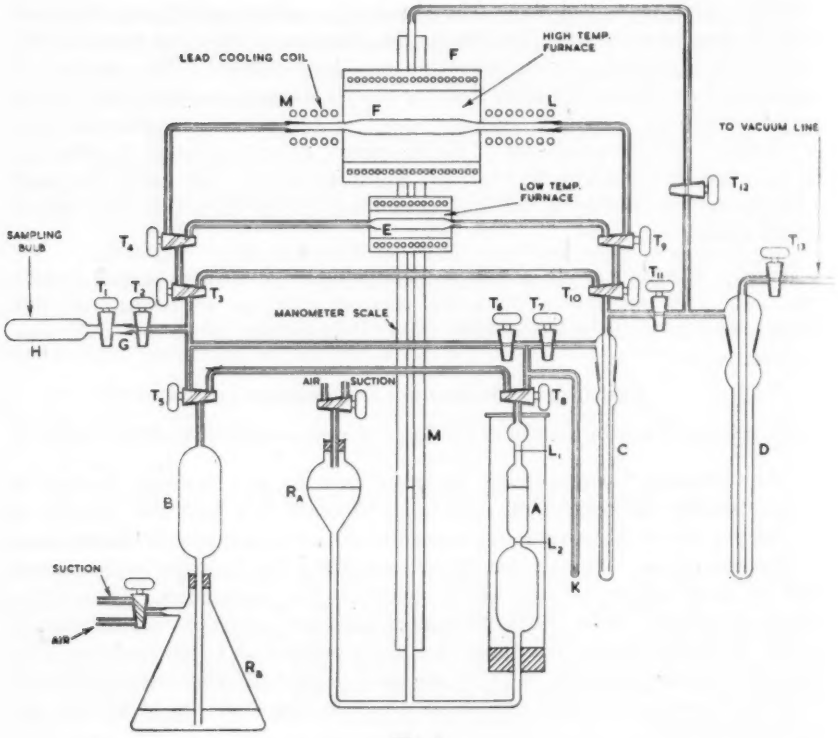


Fig. 1.
Vacuum gas analysis apparatus.

The operations involved in converting each constituent in turn to $CO_2$ can be summarised briefly as follows:—

(*i*) The gas sample is admitted to the evacuated apparatus through a trap at −80°C.

(*ii*) Any hydrocarbons condensed in the trap are estimated by distilling, circulating over CuO at 800°C. and measuring the $CO_2$; the water formed in this and subsequent operations is condensed in a trap at −80°C.

(*iii*) The gas pressure is measured in a known volume.

(*iv*) The $CO_2$ content of the exhaust gas sample is estimated by circulating the sample through a liquid-air trap and subsequently measuring the $CO_2$ after removal and storage of the uncondensed gases.

(*v*) Any hydrocarbons which remain uncondensed at −80°C. but which

condense with the $CO_2$ are estimated by passing the $CO_2$ over CuO at 800°C. and measuring the increase in pressure.

(*vi*) The CO in the uncondensed gases from (*iv*) is then oxidised to $CO_2$ over CuO at 320-330°C. The hydrogen is oxidised at this stage but is not measured.

(*vii*) The $CH_4$ is similarly estimated by oxidation at 1,000°C. The oxygen content can also be determined at this stage by absorption by free copper.

(*viii*) The residual gas is nitrogen.

*Advantages*

(*a*) The fact that the $CO_2$ produced by each constituent is measured directly by the pressure it exerts in a fixed volume, instead of by the difference between two large quantities after absorption, means that small amounts can be measured very accurately.

(*b*) The absence of liquid absorbents.

(*c*) The accuracy of the method can be adjusted to suit the quantity to be determined, by alteration of the volume in which the final pressure is measured.

*Disadvantages*

(*a*) Time required. For the complete analysis as described, and using a mercury manometer to measure pressure, the time required is 3 to 3½ hours. This time can be shortened if it is only necessary to determine $CO_2$ combustion efficiency; the analysis then takes less than 2 hours.

(*b*) Omission of hydrogen determination. Hydrogen can be estimated by measuring the contraction of a sample after oxidation on a platinum spiral, but to measure such a small quantity accurately would require a more sensitive pressure measuring device and this would increase the time required for a complete analysis to impracticable dimensions. Accordingly, in the present work, the hydrogen determination is omitted.

As normally hydrogen is less than 0.1 per cent. by volume, this omission is not serious, but it must be emphasised that it is only permissible for certain work. General comparative work will be little affected. As will be mentioned later, an alternative method for hydrogen determination is being developed which will repair the omission in the vacuum method.

*Accuracy*

The normal accuracy is $\pm 0.005$ per cent. for any carbon-containing gas, $\pm 0.01$ per cent. for oxygen, and $\pm 0.05$ per cent. for hydrogen. This corresponds to the estimation of $CO_2$ combustion efficiencies to $\pm 0.2$ per cent. at an air/fuel ratio of 60/1.

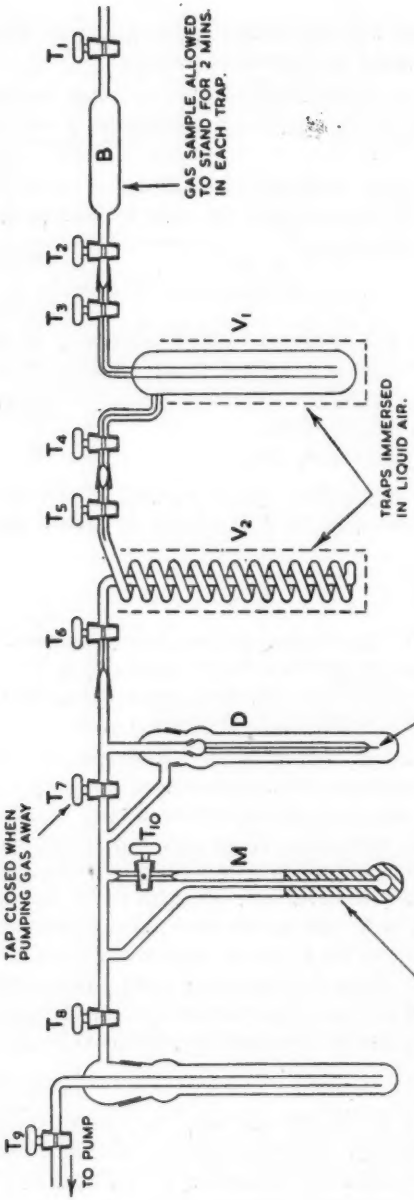


Fig. 2(*a*).

Modified Cambridge vacuum gas analysis apparatus. Apparatus for extraction of $CO_2$.

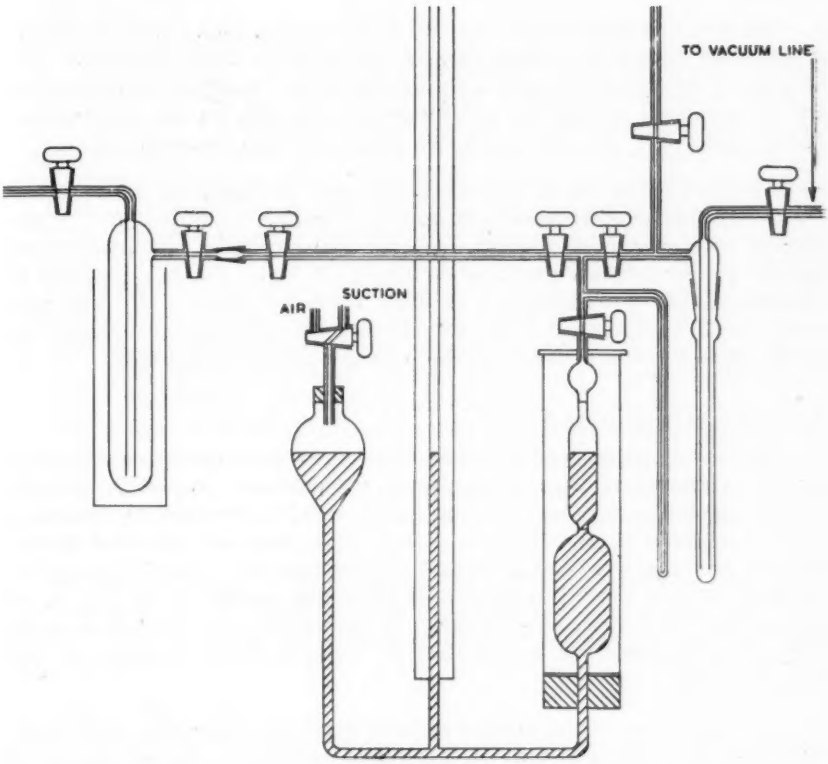


Fig. 2(*b*).
Modified Cambridge vacuum gas analysis apparatus. Apparatus for measurement of $CO_2$.

### 3.2. *Modified Cambridge vacuum methods*

As mentioned above, one of the chief disadvantages of the Cambridge vacuum method is the time required even for the determination of $CO_2$ combustion efficiency. Accordingly, special attention has been paid to modifying the original method so as to reduce the time while retaining the accuracy.

The method finally adopted[4] is to draw the gas by means of a vacuum pump from a sample bulb of known volume through a trap cooled in liquid air (*see* Fig. 2). The rate of evacuation is carefully controlled by means of a capillary restriction. After complete evacuation of the system the trap containing the $CO_2$ is transferred to another apparatus where the $CO_2$ is vaporised and the pressure it exerts in a fixed volume is measured. By this means the time-consuming circulation processes of the original vacuum method are eliminated.

The time for a single analysis is about 30 minutes, but when a series of analyses is performed together the average time for one analysis is about 20 minutes. The accuracy of the method is at least as good as that of the Cambridge vacuum method and in many cases is better, *i.e.* $\pm 0.001$ per cent. absolute for low concentrations of $CO_2$, and $\pm 0.25$ per cent. of the $CO_2$ present for high concentrations.

An extension of the above method has been developed for the estimation of CO. The gas, after the removal of the $CO_2$, is passed over CuO at 350°C., then through another trap immersed in liquid air and finally, to the vacuum pump through another capillary restriction to control the flow. The $CO_2$ produced by oxidation of the CO is measured in the same way as the original $CO_2$. This rapid method could be developed further to estimate other carbon-containing gases, but it still suffers from the disadvantage that hydrogen cannot be measured.

### 3.3. pH-*meter method*

This method, although developed before the rapid vacuum method was available for $CO_2$ determination, has now been largely replaced by it. Briefly, the principle of the method is to bubble the exhaust gas through N/1000 $NaHCO_3$ solution in which is immersed a glass electrode. This solution forms one arm of an electrolytic cell, the other arm being a standard calomel electrode. The pH value of the $NaHCO_3$ solution, which is a function of the partial pressure of the $CO_2$ in the exhaust gas, is determined on a pH-meter. A calibration curve of pH value against $CO_2$ partial pressure can be obtained by passing known amounts of $CO_2$ through the cell.

The method has the advantages of being rapid and continuous in operation. The main disadvantage is that the calibration occasionally changes because of electrical instability inherent in the present design of the cell system.

The accuracy of the method is $\pm 2$ per cent. of the actual amount of $CO_2$ in the sample under test, *i.e.* for a sample containing 2.0 per cent. $CO_2$ the absolute accuracy would be $\pm 0.04$ per cent. The instrument is thus capable of determining small amounts of $CO_2$ (*i.e.* in combustion loss) to a high degree of absolute accuracy but it is not as suitable for larger amounts.

For determination of $CO_2$ combustion efficiency the time required is 5 to 10 minutes. A more detailed analysis can be made (*i.e.* for CO, $CH_4$, $CO_2$, etc.) by having three or more separate solutions and converting in turn each of these gases to $CO_2$, as in the vacuum method.

### 3.4. *Other methods*

Other methods are either being developed or are under consideration, and the following notes are intended to indicate the potentialities of each method.

(*i*) *The Poole Combustimeter*[5]

This instrument is essentially a Wheatstone bridge, with a catalytic wire as resistance in one arm and a compensating non-catalytic wire as resistance in another arm. Provided that the temperature of the catalytic wire exceeds 600°C. all combustible gases will be oxidised at the surface, but if the temperature is below 600°C., the method may be made selective for various gases. The heat of combustion released at the wire throws the bridge out of balance by an amount proportional to the concentration of "combustible" and its heat of combustion. The main interest in the instrument is that it furnishes an accurate method for the estimation of hydrogen. Provided that the temperature of the filament is kept below 300°C. the only constituents of combustion chamber exhaust gases which react are $H_2$ and CO and, up to the present, it has been impossible to separate the response of these two gases. Nevertheless, as CO can be estimated by an independent method the hydrogen can be found by difference. This will not affect the accuracy for $H_2$ as the instrument is much less sensitive to CO. The instrument is capable of giving a full-scale deflection for 0.88 per cent. hydrogen. This corresponds to a probable accuracy of $\pm 0.005$ per cent. assuming the scale can be read to half a division.

The great advantage of the method is that it is rapid and continuous. One disadvantage is that the apparatus must be initially calibrated, which means that provision must be made for preparing mixtures of hydrogen and air with high accuracy.

(*ii*) *Conductivity methods*

Some work has been done on the development of a conductivity method for the estimation of hydrogen but it was found that for the accuracy required ($\pm 0.005$ per cent.) the instrument zero was insufficiently stable. This was probably because of the difficulty of maintaining the temperature of the incoming gas flow within a few hundredths of a degree centigrade.

As the combustimeter is arranged to overcome this, it has now superseded the conductivity method in the present development programme.

(*iii*) *Infra-red gas analyser*

An instrument which appears to have great possibilities in this field is the infra-red gas analyser. In this instrument infra-red radiation is passed through a cell containing the sample under test and then to a detector cell containing only the constituent which is to be determined. A second identical beam of infra-red radiation passes through a second system, identical to the first except that the cell which contains the sample is replaced by one containing a standard non-absorbing gas (air free of $CO_2$). The amounts of radiation received by the two detector cells will obviously differ by an amount which is equal to that absorbed by the relevant constituent in the sample and therefore proportional

to the concentration of this constituent. This differential effect is amplified and measured by an appropriate electrical circuit. The advantages of this instrument are its great accuracy (full-scale deflection for 0.03 per cent. $CO_2$ if necessary), its almost instantaneous response and its continuity. The gases in the exhaust which may be determined by means of this instrument are $CO_2$, CO, $CH_4$ and other hydrocarbons. Hydrogen, not absorbing in the infra-red region of the spectrum, is of course not estimated.

Making allowance for the full development of these various methods, it appears probable that analysis of the exhaust gas in determinations of combustion efficiency will be best effected by the use of a combustimeter in conjunction with the infra-red gas analyser. This will enable an analysis to be performed accurately, continuously, and rapidly.

In this review, mention should be made of one other method which has been used extensively, namely the National Gas Turbine Establishment gravimetric method. This method uses fractional combustion at various controlled temperatures to convert each constituent to carbon dioxide and water. These products are then estimated gravimetrically by absorbing the $CO_2$ with soda asbestos and the water with anhydrone (magnesium perchlorate) and measuring the increase in weight. The various stages of combustion are similar to those used in the Cambridge vacuum method, the essential difference between the two techniques being in the method used to measure the combustion products.

Further details of the gravimetric method may be obtained from the reference quoted[2].

## 4. SAMPLING AND INTERPRETATION OF RESULTS

With adequate analytical methods available, the most important problem remaining lies in extracting a sample which shall be representative of the exhaust gases; unless this requirement is satisfied, the overall accuracy of combustion efficiency assessment will suffer.

In assessing efficiency it is the heat release within the combustion chamber which must be measured; any delayed energy release (the simplest case of this being a long flame), occurring beyond the outlet section of the chamber normally coinciding with the turbine blades, does not contribute to the most efficient working of the engine, and hence should not be included when computing efficiency. It follows that, in sampling, any delayed reaction occurring in the combustion chamber efflux gases should be arrested at the appropriate point; this can be accomplished for all practical purposes by chilling, or reducing gas temperature to a value where reaction is impossible, or at least extremely slow.

Two courses are open, then, in obtaining the sample. Either some means must be provided for withdrawing at the outlet of the chamber, and immediately chilling,

a number of samples which when mixed provide a mean sample of the total exhaust gases; or the whole of the exhaust gases must be chilled on leaving the combustion chamber and sampled at some point downstream where they have mixed and are uniform in composition. Both practices have been followed at various establishments and each has its own particular merit and disadvantage.

Of equipment for sampling directly at the combustion chamber outlet, perhaps the most successful design in current use is that developed at the National Gas Turbine Establishment[2]. This consists of a water-cooled sampling manifold pierced with a number of holes through which the sample is metered, the whole manifold being swept at constant angular velocity back and forth across the outlet section of the combustion chamber. By suitable adjustment of the sampling conditions the amount of gas admitted through any hole is made proportional to the local mass flow of gas, and thus the device supplies a sample truly representative of the areas swept by the holes. This equipment has proved satisfactory in operation where concentration gradients across the section sampled are relatively small, but where such is not the case, the fact that in effect the sample is drawn from a finite number of narrow arcs limits its performance. A logical development of this apparatus might be a single sampling tube which is made to scan completely the combustion chamber outlet (*cf.* television practice); mechanical difficulties may be discouraging but the construction of such equipment would be amply justified in some circumstances.

Where gas composition varies widely across the outlet of the chamber perhaps the only satisfactory solution of the sampling difficulty lies in thoroughly mixing at first the whole of the exhaust gases and then withdrawing suitable quantities for analysis from a single sampling tube mounted at a convenient point downstream. As already stated, under certain conditions the use of this technique necessitates the chilling of the whole of the exhaust gases at the outlet of the chamber on test, and this problem has been tackled by injecting water from a grid of perforated pipes directly into the gas stream at a plane normally occupied by the turbine blading. The main problem involved is the design of a suitable gas mixer; the type in use at Thornton Research Centre was the outcome of trial and error; duct sections, baffles, etc., were modified and changed until gas composition across the exhaust pipe was found to be substantially uniform. A diagram of the sampling gear finally adopted is given in Fig. 3.

Both the methods of sampling outlined above suffer from one important limitation—where unburnt liquid fuel is present in the exhaust a truly representative sample cannot be collected. Thus the procedure followed for the practical determination of combustion efficiency varies according to the nature of the exhaust, *i.e.* whether it is entirely gaseous, or mainly gaseous but with some liquid fuel present. Experience has shown that at efficiencies below 85 per cent. the combustion loss will often include liquid fuel, and in order that the appropriate sampling procedure

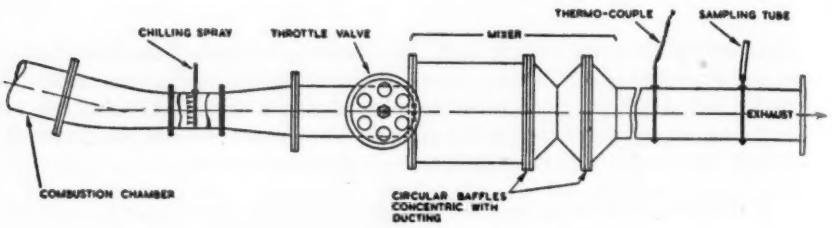


Fig. 3.
Gas sampling gear at Thornton Research Centre.

may be selected a rough approximation of efficiency is required. This can be obtained by estimating the temperature rise in the combustion chamber by means of a single thermo-couple mounted in the exhaust of the gas mixer (*see* Fig. 3). In view of the distinct differences in the techniques applied for the two exhaust conditions, it is proposed to deal separately with each.

### 4.1. *The determination of efficiency when exhaust products are wholly gaseous at the sampling temperature*

It is under these conditions that gas analysis methods of efficiency measurement are most accurate. Errors are governed only by the precision of analytical methods, the extent to which they are used, and the care taken in ensuring that the sample is truly representative of the exhaust gases; each of these factors, to a large extent, can be adjusted to suit the requirements of the test in hand. No measurements of combustion chamber air or fuel flows are necessary for the calculation of efficiency, because all data required are obtained from the analytical results.

As already stated, the greater part of the combustion loss in conventional aircraft-type chambers will be accounted for by CO and unburnt hydrocarbons and, by neglecting the loss from any free hydrogen present in the exhaust (a step often, but not always, justified), two simple approximations to combustion efficiency may be determined; these are $CO_2$ combustion efficiency, already defined, and a closer approximation to true efficiency in which allowance is made for the liberation of heat in the formation of CO.

$CO_2$ combustion efficiency may be determined by taking two samples, one (*a*) of the untreated exhaust gases, and one (*b*) of the exhaust gases treated in such a manner as first to remove $CO_2$ resulting from combustion in the test chamber, and then to oxidise unburnt carbon-containing constituents to $CO_2$. It is usually convenient to install apparatus for treating sample (*b*) adjacent to the sampling gear, and a diagram of the necessary equipment is given in Fig. 4 with explanatory notes. Both samples (*a*) and (*b*) are examined for $CO_2$ content by one of the methods already outlined, the choice being governed by the speed and accuracy required.

Then if $CO_2' = CO_2$ in sample (*a*) expressed as percentage by volume of dry gas
and $CO_2'' = CO_2$ in sample (*b*) expressed as percentage by volume of dry gas

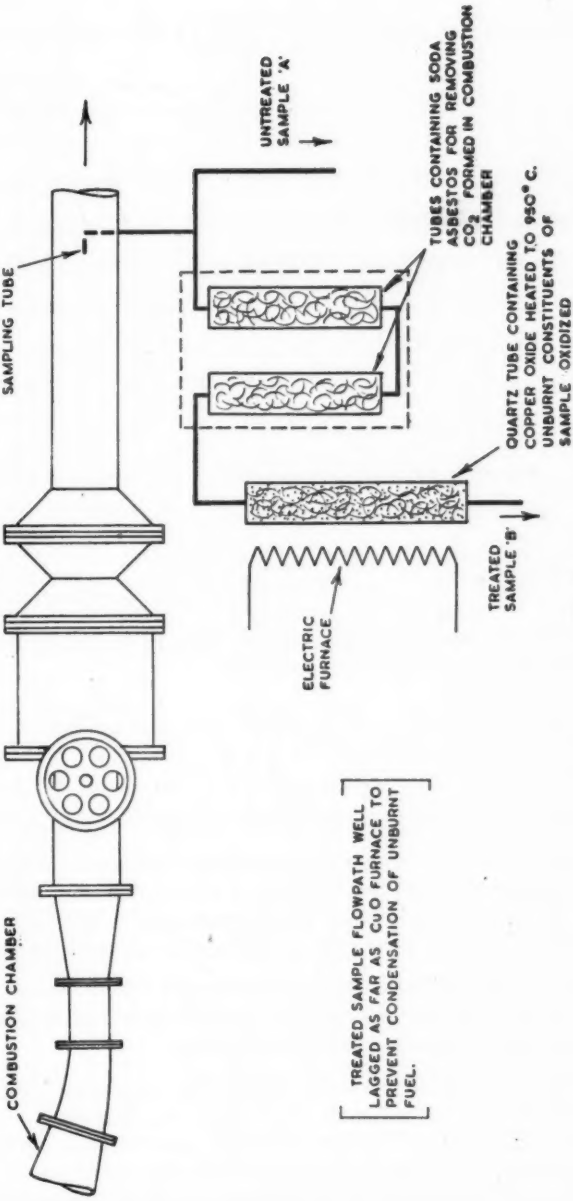
SAMPLING TUBE
UNTREATED SAMPLE 'A'
TUBES CONTAINING SODA ASBESTOS FOR REMOVING $CO_2$ FORMED IN COMBUSTION CHAMBER
QUARTZ TUBE CONTAINING COPPER OXIDE HEATED TO 950° C. UNBURNT CONSTITUENTS OF SAMPLE OXIDIZED
TREATED SAMPLE 'B'
ELECTRIC FURNACE
COMBUSTION CHAMBER
TREATED SAMPLE FLOWPATH WELL LAGGED AS FAR AS CuO FURNACE TO PREVENT CONDENSATION OF UNBURNT FUEL.

Fig. 4.
Apparatus for treating exhaust samples "on site."

$$\text{CO}_2 \text{ combustion efficiency} = \left[\frac{\text{CO}_2'}{\text{CO}_2' + \text{CO}_2''}\right] \times 100 \text{ per cent.} \quad (1)$$

$$= \left[1 - \frac{\text{CO}_2''}{\text{CO}_2' + \text{CO}_2''}\right] \times 100 \text{ per cent.} \quad (2)$$

In (2), $\frac{\text{CO}_2''}{\text{CO}_2' + \text{CO}_2''} \times 100$ per cent.—the $\text{CO}_2$ combustion loss—may have resulted from either CO, hydrocarbons, or both, and hence cannot be interpreted directly as a thermal or energy loss. The closer approximation to true combustion efficiency, allowing for the proportions of CO and hydrocarbons in the combustion loss, can be determined by following the same sampling procedure as for $\text{CO}_2$ combustion efficiency but by analysing sample (*a*) for CO, as well as for $\text{CO}_2$ content, again by one of the methods described.

Then if $\text{CO}_2''' = \text{CO}_2$ produced by oxidation of CO in sample (*a*), expressed as a percentage by volume of dry gas:—

$$\text{Combustion efficiency} = \left[1 - \frac{(\text{CO}_2'' - \text{CO}_2''') + k_1\text{CO}_2'''}{\text{CO}_2' + \text{CO}_2''}\right] \times 100 \text{ per cent.} \quad (3)$$

Where $(\text{CO}_2'' - \text{CO}_2''')$ is proportional to the loss from hydrocarbons, and $k_1\text{CO}_2'''$ is proportional to the loss from carbon monoxide.

The combustion loss $\left[\frac{(\text{CO}_2'' - \text{CO}_2''') + k_1\text{CO}_2'''}{\text{CO}_2' + \text{CO}_2''}\right]$, may be interpreted as an energy loss.

$k_1$ is a constant for any particular fuel and is calculated as shown in Appendix I.

The assumptions made in representing combustion efficiency by the expression (3) are that combustion loss from free hydrogen in the exhaust is negligible, and that the mean calorific value of the unburnt hydrocarbons (which may include cracked fuel, fuel residues, methane, etc.) is equal to the calorific value of the fuel burnt.

A practical comparison between $\text{CO}_2$ combustion efficiency and the closer approximation to true efficiency is afforded by Table I, which shows typical results of tests on an aircraft gas turbine combustion chamber.

For the most accurate measurement of efficiency consistent with reasonable rapidity, and neglecting only the small losses caused by intermediate combustion products and free carbon where present, hydrogen must be added to the exhaust constituents estimated. This can be accomplished by the use of one of the rather slow classical methods of gas analysis (*e.g.* Haldane) or by the gravimetric technique

TABLE 1

COMPARISON OF $CO_2$ COMBUSTION EFFICIENCY WITH CLOSER APPROXIMATION TO TRUE COMBUSTION EFFICIENCY ALLOWING FOR HEAT OF FORMATION OF THE CO PRESENT IN EXHAUST

*(Experiments with three different fuels)*

| *Engine speed** (Percentage of maximum) | FUEL A | | FUEL B | | FUEL C | |
|---|---|---|---|---|---|---|
| | $CO_2$ *Efficiency per cent.* | *Closer approximation to efficiency, per cent.* | $CO_2$ *Efficiency per cent.* | *Closer approximation to efficiency, per cent.* | $CO_2$ *Efficiency per cent.* | *Closer approximation to efficiency, per cent.* |
| 100 per cent. | 98.7 | 99.0 | 98.9 | 99.2 | 98.4 | 98.7 |
| 66 per cent. | 96.6 | 97.5 | 97.0 | 98.0 | 96.6 | 98.0 |
| 48 per cent. | 93.5 | 95.2 | 93.6 | 95.7 | 94.8 | 96.6 |
| 31 per cent. | 82.7 | 85.5 | 72.6 | 75.5 | 86.5 | 89.6 |

* Rig test conditions were adjusted to simulate engine conditions at various gas turbine shaft speeds.

used successfully at the National Gas Turbine Establishment[2]. Rapid methods are under development at Thornton and particular attention is being given to the use of the Poole combustimeter for this purpose.

Where, then, $H_2$ is the hydrogen content of the exhaust, expressed as a percentage by volume of the dry exhaust gases:—

$$\text{Combustion efficiency} = \left[1 - \frac{k_2 H_2 + k_1 CO_2''' + (CO_2'' - CO_2''')}{CO_2'' + CO_2'}\right] \times 100 \quad \text{per cent.}$$

For the calculation of $k_1$ and $k_2$, constants for any particular fuel, the reader is referred to Appendix I.

### 4.2. *Determination of combustion efficiency when combustion chamber exhaust products contain liquid fuel*

Under these conditions it is virtually impossible to obtain a representative sample of the exhaust because of the non-uniform distribution of liquid fuel—some may be in the form of widely-spaced droplets in the exhaust stream and some may be dribbling along the walls of the combustion chamber. Thus any analytical results from sample (*b*) would be meaningless. Fortunately, the presence of liquid fuel will not affect the sampling of the gaseous constituents of the exhaust, and $CO_2$, CO and $H_2$ may still be measured accurately. The air/fuel ratio at which the chamber is operating, or the total potential $CO_2$ in the exhaust ($CO'_2 + CO_2''$), can no longer be calculated directly from the gas analysis data, and it becomes necessary to determine this ratio by the conventional method of measuring air and fuel flow rates separately. Every precaution should be taken to ensure accuracy in these measurements in order to avoid errors in the assessment of efficiency.

To determine $CO_2$ combustion efficiency under these conditions the untreated exhaust gas sample is taken and examined for $CO_2$ content.

Then if $CO_2^t$ is the theoretical percentage $CO_2$ content of the dry exhaust gases for complete combustion, calculated from the combustion chamber operating air/fuel ratio and the carbon/hydrogen ratio of the fuel:—

$$CO_2 \text{ combustion efficiency} = \frac{CO_2'}{CO_2^t} \times 100 \quad \text{per cent.}$$

In determining the closer approximation to true combustion efficiency, taking into account the proportions of CO and hydrocarbons contributing to the combustion loss, sample (*a*) is taken and analysed for both CO and $CO_2$ as before. Whence:—

$$\text{Combustion efficiency} = \left[1 - \frac{(CO_2^t - CO_2' - CO_2''') + k_1 CO_2'''}{CO_2^t}\right] \times 100 \quad \text{per cent.}$$

Again, for maximum accuracy allowance must be made for any free hydrogen in the exhaust gases. Methods similar to those already suggested for liquid-free exhaust gases may be applied to a sample of untreated exhaust gas. Whence:—

$$\text{Combustion efficiency} = \left[1 - \frac{k_2 H_2 + k_1 CO_2''' + (CO_2^t - CO_2' - CO_2''')}{CO_2^t}\right] \times 100 \quad \text{per cent.}$$

Difficulty will be experienced sometimes in deciding whether or not the exhaust gases are free of liquid fuel. In such cases it is better to assume that they are and to sample accordingly; results of analyses will show whether sample (*b*) was valid, for if so $CO_2' + CO_2''$ will be equal to $CO_2^t$ within the limits of accuracy of the measurements taken.

It has already been stated that the choice of analytical methods for estimating the important constituents of the exhaust will be governed mainly by the required speed and accuracy of efficiency determination. For guidance in this choice Table II has been prepared, which summarises limits of accuracy of the various methods considered, together with the time required for each determination.

TABLE II

COMPARISON OF ANALYTICAL METHODS WITH RESPECT TO ACCURACY AND TIME REQUIRED

| *Method* | *Accuracy and time required for determination of*: | | |
|---|---|---|---|
| | CO | $CO_2$ | $H_2$ |
| pH | 2 per cent. of recorded CO 5-10 minutes | 2 per cent. of recorded $CO_2$ 5-10 minutes | |
| Infra-red gas analyser (estimated) | At least as good as ±0.005 per cent. absolute. Continuous | | |
| Combustimeter | | | ±0.005 per cent. absolute Continuous |
| Cambridge vacuum | ±0.005 per cent. absolute 40 minutes | ±0.005 per cent. absolute 50 minutes | |
| Modified vacuum | ±0.005 per cent. absolute 15 minutes* | ±0.005 per cent. absolute 20 minutes* | |

* N.B.—By using two sets of measuring apparatus, the CO and $CO_2$ can be measured simultaneously by the modified method. The time for an analysis for CO and $CO_2$ is then 25 minutes.

## 5. POSSIBLE FUTURE APPLICATIONS

The techniques described have been devised primarily for the purposes of laboratory rig tests where such equipment as gas chilling gear, mixing ducts, traversing samplers, etc., can be readily accommodated. Nevertheless, the methods have some possible applications in full-scale engine and field experiments where, in any case, other means of assessing combustion efficiency are often impracticable. In many instances, chilling of the exhaust gases at the plane of the turbine blades will be unnecessary, for in a well-developed combustion chamber chemical reaction beyond the turbine will rarely be observed; further, the passage of the gases through nozzle and turbine blading and thence into the jet pipe results in such turbulence that the prospects of producing a reasonably uniform gas mixture in jet or exhaust pipe are good. Thus, on engine test beds equipped with air and fuel measuring apparatus, methods similar to those already described could be adopted for efficiency determination, samples being taken from a number of stations in the engine exhaust pipe and subsequently mixed. In the field, and where exhaust products are wholly gaseous, the apparatus required for collecting samples necessary for efficiency assessment will be relatively simple and easily fitted to experimental aircraft. Unfortunately, under flight conditions giving rise to very low combustion efficiency and large quantities of unburnt fuel in the exhaust, sampling difficulties at present complicate the application of gas analysis as a means of efficiency determination, for under such conditions fuel and air flow rates cannot be measured readily with accuracy.

## ACKNOWLEDGMENT

In conclusion the authors would like to thank the Directors of Shell Refining & Marketing Co. Ltd., and also the Ministry of Supply, for permission to publish this work.

## REFERENCES

1. LLOYD, P. (1945). Experimental Work at the National Gas Turbine Establishment. Unpublished.

2. LLOYD, P. (1948). The Determination of Gas Turbine Combustion Chamber Efficiency by Chemical Means. *Transactions of the American Society of Mechanical Engineers*, May 1948, Vol. 70, No. 4, p. 335.

3. BAMFORD, C. H., and BALDWIN, R. R. (1942). A Method for the Accurate Analysis of Gaseous Mixtures. *Journal of the Chemical Society*, Jan. 1942, p. 26.

4. BALDWIN, R. R. (1947). A Rapid and Accurate Method for the Estimation of Carbon Dioxide. Thornton Research Centre Report No. R.200/47.0. (To be published in the *Journal of the Chemical Society*.)

5. POOLE, R. (1948). The Design, Testing and Calibration of a Combustible Gas Detector. *Journal of the Institution of Electrical Engineers*, June 1948, Vol. 95 (ii), p. 258.

## APPENDIX I

### *Calculation of combustion efficiency from exhaust gas analysis*

Let percentage by volume of CO in exhaust gases $= a$

Let percentage by volume of $CO_2$ in exhaust gases $= b$

Let percentage by volume of unburnt hydrocarbons in exhaust gases (expressed as $CO_2$) $= c$

Let percentage by volume of $H_2$ in exhaust gases $= d$

Consider a volume of exhaust gas equal to 22.4 litres.

Volume of CO (at normal temperature and pressure) $= \frac{a}{100} \times 22.4$ litres

Weight of CO $= \frac{28a}{100}$ grammes

Similarly, weight of $CO_2$ $= \frac{44b}{100}$ grammes

Weight of $CO_2$ from hydrocarbons $= \frac{44c}{100}$ grammes

Weight of $H_2$ $= \frac{2d}{100}$ grammes

Therefore total weight of carbon $= \frac{12\,(a+b+c)}{100}$ grammes

and total weight of fuel $= \frac{12\,(a+b+c)}{100}\,(1+h)$ grammes,

where $h$ is H/C ratio of the fuel by weight.

Similarly weight of unburnt fuel $= \frac{12c}{100}\,(1+h)$ grammes

(assuming unburnt hydrocarbons are unburnt fuel).

$\therefore$ If $K_F$, $K_H$, $K_{CO}$ are the heats of combustion of the fuel, hydrogen and carbon monoxide, respectively, expressed as calories per gramme (or CHU/lb.),

$$\text{Combustion loss} = \frac{\frac{2d}{100}K_H + \frac{28a}{100}K_{CO} + \frac{12c}{100}(1+h)K_F}{\frac{12}{100}(a+b+c)(1+h)K_F} \times 100 \quad \text{per cent.}$$

$$= \frac{2dK_H + 28aK_{CO} + 12c\,(1+h)K_F}{12\,(a+b+c)(1+h)K_F} \times 100 \quad \text{per cent.}$$

Combustion efficiency = 100 − (combustion loss).

Various approximations to the above expression can be used, as mentioned in the text.

(*a*) *Neglecting hydrogen*

Combustion loss becomes:—

$$\frac{28aK_{CO}+12c\,(1+h)\,K_F}{12\,(a+b+c)\,(1+h)\,K_F}\times 100 \quad \text{per cent.}$$

$$=\frac{\dfrac{28K_{CO}}{12\,(1+h)\,K_F}\,a+c}{a+b+c}\times 100 \quad \text{per cent.}$$

In the method of sampling used in this report,

If $CO_2'$ = percentage by volume of $CO_2$ in the untreated sample

$CO_2''$ = percentage by volume of $CO_2$ in the treated sample

$CO_2'''$ = percentage by volume of $CO_2$ from CO

$CO_2^t$ = total theoretical percentage of $CO_2$ for complete combustion derived from air/fuel ratio.

Then when exhaust products are gaseous at sampling temperature:—

$$\text{Combustion loss}=\frac{kCO_2'''+(CO_2''-CO_2''')}{(CO_2''+CO_2')}\times 100 \quad \text{per cent.}$$

$$\text{where } k=\frac{28K_{CO}}{12\,(1+h)\,K_F}$$

When exhaust products contain liquid fuel:—

$$\text{Combustion loss}=\frac{kCO_2'''+(CO_2^t-CO_2'-CO_2''')}{CO_2^t}\times 100 \quad \text{per cent.}$$

(*b*) *Neglecting hydrogen and assuming* CO *is a total loss* (*i.e.* $CO_2$ *combustion efficiency*)

When exhaust products are gaseous:—

$$CO_2 \text{ combustion loss}=\frac{CO_2''}{CO_2''+CO_2'}\times 100 \quad \text{per cent.}$$

In the presence of liquid fuel:—

$$CO_2 \text{ combustion loss}=\frac{CO_2^t-CO_2'}{CO_2^t}\times 100 \quad \text{per cent.}$$

# A SIMPLIFIED THEORY OF "SIMPLE WAVES"

by

A. GHAFFARI, Ph.D.
*(The University, Teheran)*

SUMMARY

This note is concerned with a general and exact solution of the two-dimensional equations of motion of a compressible fluid, which is steady, irrotational and isentropic. The solution arrived at is the generalisation of the Prandtl-Meyer celebrated "wedge solution" to include an expansion around any smooth (or abrupt) convex boundary.

We shall obtain the solution of equations for the most general type of motion in which the Cartesian components of velocity are connected by some functional relation throughout the field of flow.

Taking into account the conditions of continuity, zero rotation and Bernoulli's equation, together with the fundamental assumption, which implies that the components of fluid velocity are each a function of fluid speed only, it is found that the motion is necessarily *supersonic*.

It is shown that the lines of equal speed, pressure (isobars) and density are all *straight lines*, although they are not necessarily concurrent as in the original Prandtl-Meyer theory, and further that the component of fluid velocity perpendicular to the isobar is equal to the local velocity of sound.

The extended Prandtl-Meyer solution for the flow past an arbitrary fixed boundary is obtained analytically.

---

This note is concerned with the plane motion of a compressible fluid, which is steady, irrotational and isentropic. It is proposed to obtain the most general type of flow in which there is a functional relation connecting the Cartesian components of velocity $u$ and $v$, valid throughout the field of flow.

This type of motion has been discussed in papers by Lees[1] and Bateman[2],

---

[The Aeronautical Quarterly, Vol. 1, August 1949]

Paper received October 1948.

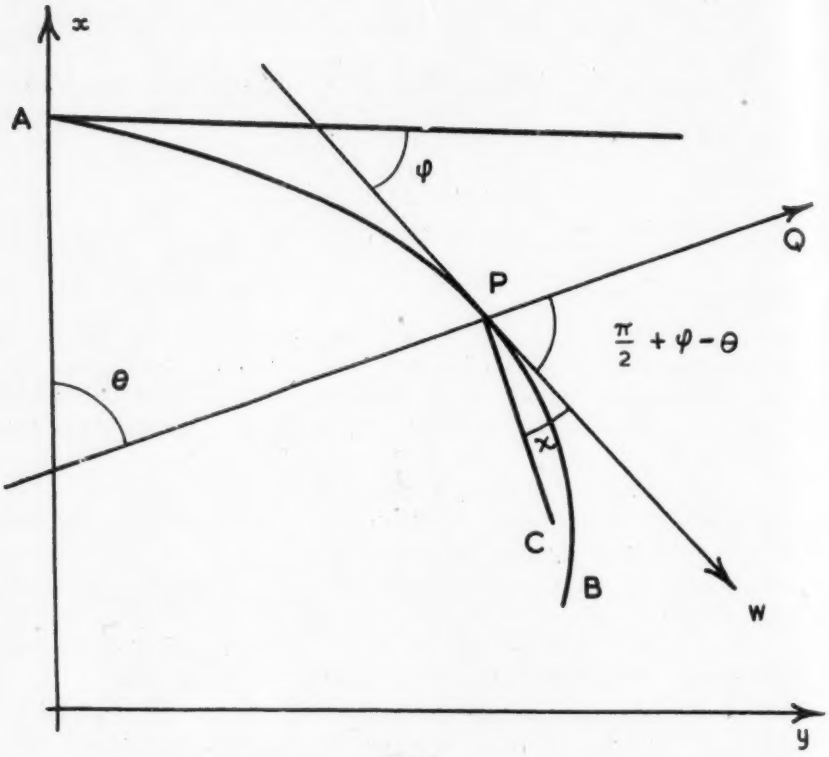


Fig. 1.

$\frac{\pi}{2} + \varphi - \theta$ is the Mach angle, AB is the stream line, PQ is the isobar, PC is perpendicular to the isobar, $w$ is the fluid velocity.

but neither investigation brings out the relation of the flow to the well-known "wedge-solution" of Prandtl and Meyer[3].

To facilitate comparison with Meyer's solution (as represented in Ref. 3), the notation of Fig. 1 is used so that

$$\left.\begin{aligned} u &= -w \sin \varphi \\ v &= w \cos \varphi, \end{aligned}\right\} \quad . \quad . \quad . \quad . \quad . \quad . \quad (1)$$

where $w$ is the fluid speed and $\varphi$ is the angular deviation of the flow from a direction parallel to the $y$-axis, measured in a clockwise direction.

The assumed functional relation between $u$ and $v$ is equivalent to the assumption that the velocity components $u$ and $v$ are each functions of the single variable $w$.

## NOTATION AND FUNDAMENTAL EQUATIONS

### *Notation*

| | |
|---|---|
| $x, y$ | rectangular co-ordinates. |
| $\theta$ | slope of isobar. |
| $\varphi$ | angle between resultant fluid velocity and $y$-axis, measured in a clockwise direction. } *see* Fig. 1. |
| $\chi$ | $\theta - \varphi$. |
| $\rho$ | density of fluid. |
| $p$ | static pressure. |
| $F, G$ | functions defined for equations (10), (11) and (12). |
| $u, v$ | components of fluid velocity parallel to rectangular axes of $x$ and $y$. |
| $w$ | resultant fluid speed $= (u^2 + v^2)^{\frac{1}{2}}$. |
| $\phi$ | potential function. |
| $\psi$ | stream function. |
| $\gamma$ | adiabatic index $= 1.4$ (for air). |
| $\lambda$ | $\{(\gamma - 1)/(\gamma + 1)\}^{\frac{1}{2}}$ |
| $a$ | local speed of sound. |
| $a_0$ | speed of sound at stagnation point. |
| $w_m$ | maximum which can be attained by fluid speed when $p=0$, $\rho=0$, and $a=0$. |

### *Fundamental equations*

The fundamental equations are given in the form

$$(\rho u)_x + (\rho v)_y = 0 \quad \text{(equation of continuity)}, \quad . \quad . \quad . \quad (2)$$

$$u_y = v_x \quad \text{(condition of no vorticity)}, \quad . \quad . \quad . \quad (3)$$

using suffixes, here and elsewhere, to denote partial (or total) derivatives.

The standard pressure-density relation for a perfect gas is not assumed until the end of this investigation (*i.e.* from equation (13)). The main results are independent of this special assumption.

Since Bernoulli's equation can be written in the form

$$a^2 \frac{d\rho}{\rho} = -w dw \quad . \quad . \quad . \quad . \quad . \quad . \quad (4)$$

the equation of continuity (2) becomes

$$u_x + v_y = -(u\rho_x + v\rho_y)/\rho = (uw_x + vw_y)\, w/a^2.$$

whence $$u_w w_x + v_w w_y = (uw_x + vw_y)\,(w/a^2),$$

or $$w_x (u_w - uw/a^2) + w_y (v_w - vw/a^2) = 0. \quad . \quad . \quad . \quad (5)$$

The condition for irrotational flow (3) becomes

$$u_w w_y = v_w w_x. \quad . \quad . \quad . \quad . \quad . \quad (6)$$

Hence, from the two equations (5) and (6)

$$u_w (u_w - uw/a^2) + v_w (v_w - vw/a^2) = 0,$$

or

$$u_w^2 + v_w^2 = (uu_w + vv_w)\,(w/a^2)$$
$$= \tfrac{1}{2}\,[d\,(u^2 + v^2)/dw]\,(w/a^2) = w^2/a^2. \quad . \quad . \quad . \quad (7)$$

Now from (1)

$$\left.\begin{aligned} u_w &= -\sin\varphi - w\,\varphi_w \cos\varphi \\ v_w &= \cos\varphi - w\,\varphi_w \sin\varphi \end{aligned}\right\} \quad . \quad . \quad . \quad . \quad . \quad (8)$$

and

Therefore

$$u_w^2 + v_w^2 = 1 + w^2 \varphi_w^2.$$

Hence from (7)

$$1 + w^2 \varphi_w^2 = w^2/a^2$$

or

$$\left(\frac{d\varphi}{dw}\right)^2 = (w^2 - a^2)/w^2 a^2. \quad . \quad . \quad . \quad . \quad (9)$$

It is clear from the last equation that $w^2 \geqslant a^2$, that is to say $w$ cannot be less than $a$, *i.e.* the motion is *supersonic* everywhere.

Before integrating equation (9) it is convenient to determine the main features of the motion. If we write

$$F = -\phi + xu + yv,$$

where $\phi$ is the velocity potential, then

$$F_x = -\phi_x + u + xu_x + yv_x = (xu_w + yv_w)\, w_x,$$

and

$$F_y = -\phi_y + v + xu_y + yv_y = (xu_w + yv_w)\, w_y.$$

Therefore

$$F_x w_y - F_y w_x = 0, \quad \text{or} \quad \frac{\partial (F,\ w)}{\partial (x,\ y)} = 0,$$

*i.e.* $F$ is a function of $w$ only, say $F(w)$.

Hence

$$\frac{dF(w)}{dw} w_x = -\phi_x + u + (xu_w + yv_w)\, w_x,$$

or

$$\frac{dF(w)}{dw} = xu_w + yv_w, \qquad (10)$$

or

$$C = Ax + By,$$

where $A$, $B$ and $C$ are functions of $w$ only.

If $w$ = constant, the equation (10) represents a straight line. The curves of equal fluid speed $w$ are also the curves of equal density and pressure, *i.e.* they are isobars. *The isobars therefore form a system of straight lines.*

If the slope of an isobar is denoted by $\theta$, then

$$\sin\theta = -\frac{u_w}{(u_w^2 + v_w^2)^{\frac{1}{2}}} = -au_w/w, \quad \text{from (7)}$$

and

$$\cos\theta = av_w/w,$$

the signs being chosen so that $\theta$ is positive when $\varphi$ is small and positive and increases with $w$. Hence the component of the fluid velocity perpendicular to the isobar is

$$w\cos(\theta - \varphi) = v\cos\theta - u\sin\theta = (vv_w + uu_w)\, a/w = a, \qquad (11)$$

*i.e.* it is equal to the local speed of sound (Fig. 1).

Similarly, if we write

$$G = -\psi + x\rho v - y\rho u,$$

then

$$G_x = -\psi_x + \rho v + x(\rho v)_x - y(\rho u)_x$$
$$= [x(\rho v)_w - y(\rho u)_w] w_x,$$

and

$$G_y = -\psi_y - \rho u + x(\rho v)_y - y(\rho u)_y$$
$$= [x(\rho v)_w - y(\rho u)_w] w_y.$$

Therefore $G_x w_y - G_y w_x = 0$, or $\dfrac{\partial(G, w)}{\partial(x, y)} = 0$,

*i.e.* $G$ is a function of $w$ only, say $G(w)$,

and $\psi = x\rho v - y\rho u - G(w)$,

or $$\psi = \rho w (x \cos\varphi + y \sin\varphi) - G(w), \quad . \quad . \quad . \quad . \quad (12)$$

The equation of the stream lines is therefore

$$x \cos\varphi + y \sin\varphi = R(\varphi),$$

where $R(\varphi)$ is some function of $\varphi$.

$$R(\varphi) = [G(w) + \text{constant}]/\rho w.$$

Hence, if any one stream line is known, as for example a solid boundary of the fluid, then $x$, $y$, $\varphi$ are also determined everywhere as functions of $w$.

To avoid the ambiguity in sign which is implicit in (9), we determine $\varphi_w$ from the equation

$$\tan\varphi = -u/v.$$

Then

$$\varphi_w = -(vu_w - uv_w)/(v^2 \sec^2\varphi) = (w/a)(v \sin\theta + u \cos\theta)(1/w^2)$$
$$= (\sin\theta \cos\varphi - \cos\theta \sin\varphi)/a = \sin(\theta - \varphi)/a.$$

We can complete the integration in the case of a perfect gas, for which

$$a^2 = a_0^2 - \tfrac{1}{2}(\gamma - 1) w^2. \quad . \quad . \quad . \quad . \quad . \quad (13)$$

We now express $w$ and $a$ in values of the angle

$$\chi = \theta - \varphi.$$

We have

$$a = w\cos\chi, \quad \text{from (11)}$$

and, taking into account equation (13), we obtain

$$w^2 = \frac{a_o^2}{\frac{1}{2}(\gamma-1)+\cos^2\chi}, \qquad (14)$$

and

$$2\frac{dw}{w} = \frac{2\cos\chi\sin\chi\,d\chi}{\frac{1}{2}(\gamma-1)+\cos^2\chi}.$$

Hence

$$d\varphi = \frac{\sin\chi d\chi}{a} - \tan\chi\frac{dw}{w} = \frac{\sin^2\chi d\chi}{\frac{1}{2}(\gamma-1)+\cos^2\chi}$$

$$= -d\chi + \frac{\frac{1}{2}(\gamma+1)\,d\chi}{\frac{1}{2}(\gamma-1)+\cos^2\chi}.$$

Therefore

$$\varphi = -\chi + \frac{1}{\lambda}\tan^{-1}(\lambda\tan\chi), \qquad (15)$$

where

$$\lambda = \left(\frac{\gamma+1}{\gamma-1}\right)^{\frac{1}{2}},$$

since $\varphi$ and $\chi$ vanish together.

All the variables can now be expressed in terms of the angle $\chi$. For

$$\left.\begin{aligned}
\varphi &= (1/\lambda)\tan^{-1}(\lambda\tan\chi) - \chi,\\
\theta &= \chi + \varphi,\\
\tan\chi &= (1/\lambda)\tan(\lambda\theta),\\
w^2 = \frac{a_o^2}{\frac{1}{2}(\gamma-1)+\cos^2\chi} &= \frac{2a_o^2}{\gamma-1}\left[1-\tfrac{1}{2}(1-\lambda^2)(1+\cos 2\lambda\theta)\right]\\
&= \tfrac{1}{2}w_m^2\left[(1+\lambda^2)-(1-\lambda^2)\cos 2\lambda\theta\right],
\end{aligned}\right\} \qquad (16)$$

and

$$\left.\begin{aligned}
u &= -w\sin\varphi,\\
v &= w\cos\varphi,\\
a &= w\cos\chi.
\end{aligned}\right\}$$

These expressions for the components of velocity will be recognised to be identical with those of the Prandtl-Meyer "wedge-solution" with one significant

modification. The angle $\theta$ has not been assumed to be the ordinary radial co-ordinate. Hence the isobars ($\theta$=constant) are not necessarily concurrent straight lines as in the original Prandtl-Meyer solution.

We have in fact obtained analytically the extended Prandtl-Meyer solution for the flow past an arbitrary fixed boundary. To establish this we have only to show that one stream line can be prescribed arbitrarily in our solution.

Now let a stream line be given in the form

$$x=x(\varphi), \quad y=y(\varphi)$$

$\varphi$ being the direction of the tangent to the stream line.

Then the equations (14) and (16) determine $w$, $a$ and therefore $\rho$, in terms of $\varphi$ along the stream line. Equation (12) then determines the unknown function $G(w)$, and *all* the stream lines are determined.

The preceding analysis therefore furnishes a formal proof of the extended Prandtl-Meyer solution, which has hitherto been adopted as an intuitively obvious generalisation of the original "wedge-solution."

The author wishes to thank Professor G. Temple, F.R.S., for his valuable suggestions.

## REFERENCES

1. LEES, F. (1924). On a Case of Steady Flow of a Gas in Two-Dimensions. *Proc. Camb. Phil. Soc.*, Vol. 22, 1924.

2. BATEMAN, H. (1930). The Irrotational Motion of a Compressible Inviscid Fluid. *Proc. Nat. Acad. Sc.*, XVI, 1930.

3. TAYLOR, G. I., and MACCOLL, W. (1935). *Aerodynamic Theory* edited by Durand, Vol. III. Div. H., Chapter IV, 1935.